

**Phase I Clinical Trial of Recombinant Oncolytic  
Newcastle Disease Virus for Intracranial Meningioma**

Jamie Nicole King

Thesis submitted to the faculty of the Virginia Polytechnic Institute and State  
University in partial fulfillment of the requirements for the degree of  
Master of Science  
in  
Biomedical and Veterinary Sciences

John H. Rossmeisl Jr., Chair

Kemba S. Clapp

Kevin Lahmers

June 23, 2017

Blacksburg, Virginia

Keywords: Meningioma, Newcastle Disease Virus, Canine, Oncolytic Therapy

**Phase I Clinical Trial of Recombinant Oncolytic  
Newcastle Disease Virus for Intracranial Meningioma**

Jamie Nicole King

**ABSTRACT**

**(Academic)**

Meningioma is one of the most commonly diagnosed intracranial tumors in dogs and humans. Treatment failures resulting in local recurrence and death remain common in tumors of high grade, prompting a need for additional therapeutic options that are both effective and affordable.

Genetic modification of the LaSota strain of Newcastle Disease Virus (rLAS) has allowed the virus' fusion protein cleavage site to be replaced with that belonging to urokinase plasminogen activator (rLAS-uPA). This site is cleavable exclusively by the uPA receptor (uPAR), which is overexpressed in canine meningioma. The rLAS-uPA represents a targeted therapy that has the potential to be efficacious against meningioma when administered systemically.

A Phase I clinical trial was designed to evaluate the safety and preliminary efficacy of rLAS-uPA administered to dogs with presumptive intracranial meningioma. The primary endpoint was to define the safety of rLAS-uPA, as determined by serial clinical and laboratory assessments during and after viral administration, using standard toxicity metrics defined by the Veterinary Cooperative Oncology Group (VCOG)<sup>1</sup>. Secondary end-points included anti-tumor activity quantified by magnetic resonance imaging (MRI) assessment of tumor size, and characterization of immune responses to the rLAS-uPA.

Four dogs completed the trial without significant toxicity. No objective tumor responses were noted on MRI from any dog. All dogs produced antiviral antibodies and increased circulating cytokines during the course of treatment. No virus was recovered from plasma, urine, or cerebrospinal fluid. These results indicate that further investigation into the rLAS-uPA dose intensity and interval are required to further develop this therapy.

**Phase I Clinical Trial of Recombinant Oncolytic  
Newcastle Disease Virus for Intracranial Meningioma**

Jamie Nicole King

**ABSTRACT**

**(Public)**

The use of a modified Newcastle Disease Virus intravenous infusion to treat brain tumors in dogs has been shown to have no overt significant adverse effects. However, further investigation is required to determine the efficacy and optimal dosing protocol for this potential treatment.

## **DEDICATION**

In memory of Dr. Subbiah Elankumaran. Dr. Elankumaran's expertise and contribution regarding the formulation of the rLaS-uPA for use as an oncolytic agent, was invaluable to the implementation of this clinical trial.

## **ACKNOWLEDGEMENTS**

I wish to express my sincere gratitude to those individuals without whom it would not have been possible to complete this thesis. In no particular order, they are: John H Rossmeisl Jr., Harini Sooryanarain, Kemba Clapp, Kelli Hall-Manning, Kevin Lahmers, Theresa Pancotto, Karen Inzana, Maureen Sroufe, Nicky Kandzior and of course Subbiah Elankumaran.

## TABLE OF CONTENTS

<b>ABSTRACT (Academic)</b>	ii
<b>ABSTRACT (Public)</b>	iii
<b>DEDICATION</b>	iv
<b>ACKNOWLEDGEMENTS</b>	v
<b>TABLE OF CONTENTS</b>	vi
<b>LIST OF FIGURES</b>	vii
<b>LIST OF TABLES</b>	viii
<b>LIST OF ABBREVIATIONS</b>	ix
<b>CHAPTER 1: LITERATURE REVIEW</b>	1
<b>1.1 Introduction</b>	
<b>1.2 Overview of Intracranial Meningioma</b>	2
<i>a. Incidence and Pathogenesis</i>	2
<i>b. Imaging Characteristics</i>	8
<i>c. Therapeutic Options</i>	9
<b>1.3 Newcastle Disease Virus</b>	11
<i>a. Biological Behavior</i>	11
<i>b. Use as an Oncolytic Viral Agent</i>	13
<b>1.4 Urokinase Plasminogen Activator System</b>	17
<i>a. Components and General Function</i>	17
<i>b. Tumor Applications</i>	17
<b>CHAPTER 2: EXPERIMENTAL METHODS AND TRIAL PROTOCOL</b>	19
<b>2.1 Hypothesis and Specific Aims</b>	19
<b>2.2 uPAR Immunohistochemistry</b>	20
<b>2.3 Canine Eligibility and Recruitment</b>	21
<b>2.4 Assessment of Safety and Tolerability</b>	22
<b>2.5 Formulation and Dosing of the rLAS-uPA for Clinical Use</b>	24
<b>2.6 Canine Biological Sample Collection</b>	29
<b>2.7 Canine Immune Responses to rLAS-uPA Administration</b>	30
<b>2.8 Assessment of Therapeutic Responses to rLAS-uPA</b>	34
<b>CHAPTER 3: RESULTS</b>	38
<b>CHAPTER 4: DISCUSSION</b>	49
<b>CHAPTER 5: CONCLUSIONS AND FUTURE DIRECTIONS</b>	53
<b>REFERENCES</b>	x

## LIST OF FIGURES

**Figure 1:**

Photomicrographs of tropism modified and protease activated NDV in uPAR expressing canine glioma cells.

**Figure 2:**

Flow Chart depicting the rLAS-uPA dosing cohorts and schema.

**Figure 3:**

Histological images of uPAR immunoreactivity in canine meningiomas.

**Figure 4:**

Line graph plotting anti-rNDV antibody responses in dogs treated with rLAS-uPA.

**Figure 5:**

Bar graph detailing serum concentrations of TNF- $\alpha$ , IFN- $\gamma$ , and TRAIL in dogs treated with rLAS-uPA.

**Figure 6:**

Comparative pre- and post-treatment MRI images of dogs (patients) A and D demonstrating cystic foci in their tumors post-treatment.

**Figure 7:**

RT-PCR for rLAS-uPAR NDV in the tumor and blood of patient C.

## LIST OF TABLES

**Table 1:**

World Health Organization Grading Scheme A for Meningioma

**Table 2:**

World Health Organization Grading Scheme B for Meningioma

**Table 3:**

Canine rLAS-uPA Clinical Trial Workflow

**Table 4:**

Phase I, 3+3 Conventional Dose Cohort Escalation Decision Design

**Table 5:**

Canine Meningioma Patient Demographics

**Table 6:**

Adverse Events (AE) Observed During Trial

**Table 7:**

RAVNO MRI-Based Tumor Response Assessments

**Table 8:**

Clinical Outcomes of Dogs Treated in the Trial



## CHAPTER 1: LITERATURE REVIEW

### 1.1 Introduction

Intracranial meningioma is one of the most frequently documented extra-axial neoplasms of small animals and humans. The Central Brain Tumor Registry of the United States (CBTRUS) reports that meningioma accounts for about 36.7% of all tumors reported in humans.<sup>2,3</sup> Similar findings are published in veterinary literature for this tumor in dogs.<sup>4,5</sup> Definitive diagnosis of meningioma is based upon pre-established grading schemes set forth by the World Health Organization (WHO), utilizing histopathological evaluation. However, in both human and veterinary medicine, Magnetic Resonance Imaging (MRI) characteristics have been well described.<sup>6,7</sup> This imaging modality may be considered to be the most common method of presumptive diagnosis of this tumor type in veterinary medicine, given that it is less invasive than actual tumor sample retrieval, which would be required in order to make a definitive diagnosis, and that it is a widely utilized diagnostic tool in the field of veterinary neurology.

Treatment options for intracranial meningioma in veterinary patients while statistically have been shown to prolong median survival time, are rarely curative, and are often cost prohibitive to clients. These standard therapeutic interventions include surgical cytoreduction and/or external-beam radiation. Example: A routine lateral rostral craniectomy, one of the most commonly performed approaches to the skull, costs around \$5,000 with neuroimaging at the Virginia-Maryland College of Veterinary Medicine Veterinary Teaching Hospital (VMCVM VTH). Additionally, a standard course of fractionated, external beam-radiation therapy at a facility closest to the VMCVM VTH, North Carolina State University College of Veterinary Medicine (NCVU-CVM), costs about \$6,000-7,000. There are also some associated

morbidity and/or mortality risk factors to affected animals if standard therapeutic options are elected, including transient and/or permanent neurological deterioration, and radiation toxicity. Similar therapeutic options are utilized in human patients affected with this tumor.

Given the possible complications associated with standard/traditional treatment options, further investigation is warranted into less invasive, more affordable, and therapeutically-active treatment alternatives, which may be utilized to help effectively eradicate this tumor from affected individuals in both humans and multiple veterinary species.

Therefore, a Phase I Clinical Trial was designed to look more closely at the safety and potential effectiveness of intravenous administration of the known viral oncolytic agent, recombinant LaSota strain of Newcastle Disease Virus<sup>8</sup> in a small population of canines with presumptive intracranial meningioma based upon neuroimaging. The virus was genetically modified to target urokinase plasminogen activator receptor (uPAR), which has been documented in preliminary evaluation to be overexpressed in canine and human meningioma.

## **1.2 Overview of Intracranial Meningioma**

### *a. Incidence and Pathogenesis*

It is reported that Felix Plater provided the first description of a meningioma in man in 1614.<sup>9</sup> The meningioma has since that time gone on to represent one of the most commonly reported intracranial tumors in both humans and canines. According to the veterinary literature which will be the main focus of this review, intracranial meningioma has a variable reported incidence depending on the resource cited. A recent review published in *The Veterinary Journal* in 2012 acknowledges two retrospective studies from Troxel et al in 2003 and Snyder et al in 2006, which published that meningioma occurs in about 22.3% (Snyder) and 59% (Troxel) of

canine and feline patients diagnosed with intracranial neoplasia respectively. The average of these percentages is similar to what has been published in the most recent supplement of the CBTRUS in humans, with an overall distribution of about 36.2%<sup>2</sup> for this tumor from 2009-2013.

Meningioma as the name implies, is a tumor arising spontaneously from the meninges. The meninges are layers of membranous protective tissue which cover the brain and spinal cord. The tumor is believed to arise specifically from arachnoid cap cells (meningothelial cells) and granulations.<sup>4,10</sup> As such, it is given the specific descriptor of extra-axial, in regards to its location relative to the brain parenchyma. This denotes that the tumor largely resides outside of the brain, and exerts a compressive effect against the brain and/or ventricular system with growth, lending itself to clinical signs of brain dysfunction. Therefore, the descriptive term of “brain tumor” is in fact a misnomer. As a sequela to direct compression, swelling of the brain may also occur, which is termed vasogenic edema. Vasogenic edema manifests following extravasation of fluid into the interstitial space of the white matter surrounding the tumor, as a result of disturbance in the blood-brain barrier.<sup>11</sup> As edema forms and mass effect progresses, a secondary rise in intracranial pressure may occur. In the majority of cases, it is the secondary consequences of meningioma growth within the rigid construct of the calvarium, which lends this tumor its overall morbidity and mortality.

The site of origin of the meningioma will determine the manifestation of the clinical signs noted. For example, a meningioma located in the region of the rostral telencephalon (such as the frontal lobe) may result in clinical signs of seizure as it grows to apply compression to this region of the brain. Anatomical location has been used as a classification scheme for meningioma since the early twentieth century, following the publication of Dr. Harvey Cushing’s

book on meningioma with Louise Eisenhardt in 1938.<sup>12</sup> Anatomical classification nomenclature is based largely upon the location of the meninges from which the meningioma in question arises. The two most common locations reported in 1938 and in 2003, are meningioma of parasagittal and convexity origin with a frequency of about 25% and 19% respectively.<sup>12</sup> Parasagittal meningioma arises from the falx; the region of the meninges that anatomically divides the brain into right and left hemispheres. Convexity meningioma arises from the meninges adjacent to the convex surface of the calvarium and may overlie any portion of what is typically termed the dorsal surface of the skull. Many convexity meningiomas overlie the dorsally located cerebral hemispheres within the cranial fossa, such as the frontal, temporal, occipital and parietal lobes. However, convexity meningioma tumors may also arise over the meninges of the cerebellum located within the caudal fossa.

An anatomical classification scheme has also been utilized in veterinary literature, most notably by Sturges et al in 2008<sup>13</sup>, which reviewed intracranial meningiomas in 112 dogs and found that the majority of the tumors evaluated, 41/114, were located within the olfactory bulbs (termed olfactory meningioma) of the affected animals. Parasagittal (termed falcine) and convexity meningioma were noted in 18/114 animals and 7/114 animals respectively. Of note on histopathological evaluation by Sturges et al, tumors within all three groups (olfactory, parasagittal and cerebral convexity), were associated with more prominent parenchymal vasogenic edema.

In human medicine, etiologic risk-factors for the spontaneous development of meningioma have historically been identified as: exposure to ionizing radiation therapy, increased sex hormone (estrogen), and familial/genetic predisposition (neurofibromatosis).<sup>9</sup> Radiation-induced meningioma has been studied in human medicine for decades. There has been

shown to be a direct correlation between the intensity of the radiation exposure, and the onset of meningioma formation. High dose radiation exposure (> 20 Gy) results more typically in the development of radiation-induced meningioma at the site of irradiation by a mean age of 29-38 years.<sup>14</sup> Conversely, spontaneous meningioma is diagnosed in most humans at around age 66, and the predilection for development of a meningioma tumor increases with advancing age.<sup>2,3</sup>

Women are stated to be predisposed to the development of meningioma over men by a ratio of 2.27:1.<sup>2</sup> Pregnancy in women has also been noted to result in transient clinical worsening, related to the site of meningioma formation.<sup>15</sup> Erroneously, as was previously thought, meningioma tumors have been shown to lack estrogen receptors and instead express an abundance of progesterone receptors.<sup>16</sup> It is thought that increased progesterone levels (especially during the later stages of pregnancy) may contribute to increased vasodilation and secondary inflammatory responses within the brain parenchyma, although these findings continue to require research investigation validity.<sup>15</sup>

The same risk factors have not been noted in the current veterinary literature. However, the tumor is most often diagnosed in older animals, with a published median age of 11.1 years in dogs<sup>17</sup> and 12.1 years in cats.<sup>14</sup> Additionally, meningioma is more commonly found in dogs with a dolichocephalic conformation.<sup>18</sup> In 2003, Adamo et al<sup>19</sup> found that both feline and canine meningioma (15 samples evaluated) also express progesterone receptors, and mostly lack estrogen receptor expression, similar to data which is reported in humans. Interestingly, the study also showed evidence that increased expression of progesterone on meningioma tumor cells was inversely related to biological aggressiveness. Spontaneous canine and human meningioma have been demonstrated to share similar expression patterns of growth factor receptors, chromosomal deletions, and losses of function of tumor suppressor gene, such as Vascular Endothelial Growth

Factor (VEGF), and Ki-67 a cell proliferation marker.

The growth pattern for meningioma is slow in the majority of both human and veterinary patients, although biologically invasive and fast growing subtypes have been documented.

Typically, meningioma is present as a single tumor, although multiple tumors have been documented in a few patients.<sup>20,13</sup>

It is postulated that approximately 40% of spontaneous canine intracranial meningiomas display atypical or malignant phenotypes corresponding to the meningioma variants that have a propensity to recur in humans.<sup>21</sup> The most recent analysis of reported WHO classified meningioma in humans from 2009-2013 reveals that roughly 18.6% of meningioma display atypical or anaplastic characteristics.

The WHO established grading scheme for meningioma is listed as (**Table 1**):

**Table 1: World Health Organization Grading Scheme A for Meningioma<sup>4,5</sup>**

<b>WHO Grade</b>	<b>Descriptor</b>	<b>Pathological Features</b>
<b>Grade I</b>	Benign	Mitotic index < 4 mitotic figures per 10 high powered fields.
<b>Grade II</b>	Atypical	Mitotic index of at least 4 mitotic figures per 10 high powered fields. Also requires at least 3 of the following histologic features: increased cellularity, small cells with an increased nucleus to cytoplasm ratio, large nucleoli, pattern-less or sheet-like growth, and/or a focus of geographic necrosis.
<b>Grade III</b>	Malignant	Requires 2 of the following criteria: mitotic index $\geq$ 20 mitotic figures per 10 high powered fields, brain invasion, and/or frank anaplasia (sarcoma, carcinoma or melanoma like histology).

Of these grades, the majority of meningioma tumors documented in the United States are classified as Grade I.<sup>2,3</sup> It has been estimated that up to 22.6% of cats retrospectively diagnosed with intracranial neoplasia, had incidental meningioma.<sup>4,6</sup> This gives weight to the fact that the

biological behavior of this neoplasm may be unpredictable, and that those cats were likely affected with Grade I tumors. Incidental meningioma in dogs comprised only 3.4% of animals included in a retrospective assessment by Snyder et al in 2006. The discrepancy in these percentages is likely multifactorial and may speak to species specific differences in tumor etiopathogenesis.

Further characterization of intracranial meningioma is largely based upon cell morphology, as demonstrated by the guidelines set forth by the WHO, which have been extrapolated for use in characterizing both human and canine meningioma tumors (**Table 2**).<sup>22</sup> Meningioma cell morphology broadly consists of psammoma bodies and meningothelial cellular whorl formation. Psammoma bodies appear cytologically as concentric rings of necrosis surrounded by dystrophic calcification, and are not pathognomonic for meningioma tumors.<sup>23</sup> Characterization of cell morphology may be useful for predicting biological behavior of a specific meningioma as specific morphologies have been noted to correspond to WHO tumor grade (**Table 2**).

**Table 2: World Health Organization Grading Scheme B for Meningioma**

<b>WHO Grade</b>	<b>Descriptor</b>	<b>Cell Morphology Type</b>
<b>Grade I</b>	Benign	Meningothelial, Fibrous, Microcystic, Transitional Psammomatous, Angiomatous, Secretory
<b>Grade II</b>	Atypical	Atypical, Clear cell, Chordoid
<b>Grade III</b>	Malignant	Rhabdoid, Papillary, Malignant

*b. Imaging Characteristics*

i. Magnetic Resonance Imaging

Meningiomas are described as extra-axial masses, that usually occur singly. However, multiple tumors and metastases have been infrequently reported using standard MRI.<sup>6</sup> MRI is the modality of choice when assessing structural disease associated with brain parenchyma, including evaluation of the presence of extra-axial neoplasms.

To be classified as extra-axial, the mass or tumor must adhere to specific characteristics – it must reside outside of the brain parenchyma while maintaining an often, broad-based meningeal attachment and/or it must reside within the ventricular system. These characteristics are not definitive for meningioma alone, and other cancerous (i.e. histiocytic sarcoma, choroid plexus tumor, lymphoma) and non-cancerous masses may also have a similar appearance on MRI.<sup>7</sup>

On T2-weighted images where fluid and fat appear bright (hyperintense), meningioma typically appear hyper-to-isointense (similar) to grey matter (~50% of tumors in humans).<sup>24</sup> However, some tumors will appear hypointense when compared to grey matter, which may correlate to tumor calcification.

Pure fluid appears dark (hypointense) in T1-weighted images, and meningioma is typically shown as isointense to grey matter on these images; however, some retrospective imaging analyses, such as noted by Sturges et al, document a more heterogeneous appearance to meningioma, with 18% appearing hyperintense and 11% appearing hypointense using this imaging sequence. With the addition of a gadolinium-based contrast agent, homogenous and marked contrast enhancement of these tumors is seen with enhancement of the adjacent meninges causing a classic “dural tail” sign.<sup>13,25</sup>



Additionally, skeletal changes such as hyperostosis (thickening) and rarely osteolysis may also occur.<sup>6</sup> In the latter, as was reported by Rossmeisl, Kopf and Ruth in 2015, secondary transcalvarial herniation and/or bony tumor invasion may also be noted.<sup>26</sup> Bone changes often appear significantly hypointense relative to grey matter due to their inherent calcification property.

## ii. Computed Tomography

Computed Tomography (CT) is best suited for evaluation of skeletal changes within the skull and nasal cavity. However, some limited soft-tissue brain evaluation and assessment is possible within the cranial fossa as well. Given beam-hardening artifacts, it can be difficult to accurately interpret disease within the caudal fossa.

Meningioma typically appears homogenous and iso-to-hyperattenuating relative to brain parenchyma.<sup>4</sup> If calcified, the tumor will appear more hyperattenuating correlating with an increase in Hounsfield units. Calcification may impair subtle contrast enhancement, but otherwise the tumor typically enhances uniformly post-administration of an iodinated intravenous contrast agent.

Additionally, adjacent skeletal hyperostosis (thickening) may also be noted.<sup>27</sup> Similar imaging characteristics are also noted in human meningioma.

## c. *Therapeutic Options*

Surgical cytoreduction is considered the mainstay of treatment for canine meningiomas, but residual or recurrent disease following surgery remains a significant source of morbidity and mortality. This is illustrated by a reported median survival of 7 months following surgical resection.<sup>28</sup> Recent literature looking at a smaller case series utilizing a surgical aspirator during cytoreduction, found a much longer median survival time of 1,254 days.<sup>29</sup> The authors surmised

that the increased median survival time was directly related to more complete surgical tumor excision with the aid of the surgical aspirator as compared to manual cytoreductive techniques. Greco et. al. also noted a strong correlation between increasing length of median survival time and decreasing histologic tumor grade. Interestingly, the listed median survival time is subject to strong inherent bias due to the fact that it was largely based upon two patients who post-operatively received chemotherapy (hydroxyurea) and lived 999 days and 1,525 days respectively. Currently there is inconclusive data to warrant chemotherapy as an effective treatment modality of meningioma tumors in any species.<sup>30,31</sup>

Additionally, a retrospective study evaluating endoscopic-assisted surgical tumor cytoreduction by Klopp and Rao in 2009 noted a median survival time of 2,104 days for cerebrally located meningioma and 702 days for those tumors located in the caudal fossa.<sup>32</sup> The authors postulated that the increased median survival time reported for cerebral meningioma was due to enhanced visualization of gross tumor intraoperatively, also allowing for more complete excision.

In 2014, Ijiri and colleagues in Japan published a study outlining treatment and surgical times following MRI-guided microsurgical cytoreduction of meningioma tumors in 22 dogs and 1 cat.<sup>33</sup> A surgical aspirator was also used to perform tumor excision similar to that published by Greco, but unlike Greco, intraoperative MRI was utilized to help guide tumor removal to allow for a more complete gross tumor resection. The average survival time for all canines post-operatively was just under 2 years. However, one patient lived 4 years post-operatively (1,460). No data regarding tumor grade or cell morphology was reported in the study.

Radiation therapy has been demonstrated to be beneficial as both a primary and/or adjuvant treatment modality in dogs with meningioma. Median survival times listed in the

literature range from 12-18 months; however, a standardized radiation therapy protocol has yet to be established, and biological criteria of the meningioma is often not taken into consideration.<sup>28,34</sup> Hu et al, in the 2015 veterinary literature review of brain tumor treatment in dogs, were unable to comment on whether or not a specific form of radiation therapy (stereotactic, fractionated, intensity-modulated, etc.) was superior to another in their analyses due to limited amount of published data on these treatment modalities, especially in cases with confirmed histopathological conformation of meningioma.

The prognosis associated with palliative treatment of canine meningioma is generally considered to be poor. This is largely due to the severity of clinical signs at the onset of diagnosis, as tumors likely are asymptomatic in cats and dogs for some time, until the nervous system is no longer able to compensate for the insult. Overall medial survival times are reported as approximately 2 months when all tumor locations are considered. The addition of chemotherapy to palliative medications currently employed as standard of care (corticosteroids, and anticonvulsant drugs where applicable) offers no significant advantage in regards to enhancement of survival time of quality of life.<sup>35</sup>

In human medicine, a median survival time of 10 years has been documented post-surgical excision; however, this number is dependent on tumor grade and degree of surgical excision.<sup>21</sup>

### **1.3 Newcastle Disease Virus**

#### *a. Biological Behavior*

Newcastle Disease Virus, abbreviated as NDV, is an avian paramyxovirus. It is an enveloped, negative-sense, single-strand ribonucleic acid (RNA) virus, whose name is derived

from the location of the first known avian infection occurring in England in 1926.<sup>36</sup> The virus is divided into three major subcategories based upon its pathogenic behavior: velogenic (virulent), mesogenic (intermediate) and lentogenic (avirulent, “wild-type”). Lesser described pathotypes of the virus include neurotropic velogenic and asymptomatic enteric viruses.<sup>37</sup> Infected animals typically show changes in mentation, facial and wattle edema and/or gastrointestinal upset. Broiler and/or laying hen infection with Newcastle Disease Virus has, in the past, lead to significant production losses. This has prompted the implementation of successful immunization protocols, which have resulted in outbreak eradication in the United States and other countries.<sup>38</sup>

Neurological dysfunction of paralysis or torticollis is also a potential clinical sign.<sup>39</sup> NDV readily crosses the blood brain barrier by mechanisms similar to other paramyxoviruses. Acute viremia predisposes the release of cytokines and other inflammatory mediators, which result in disruption of endothelial tight junctions and an overall increase in vascular permeability and viral passage into the central nervous system.<sup>40</sup>

A major determinant of virulence in Newcastle Disease Virus is the fusion (F) protein. It is thought that NDV encodes for at least six major proteins which aid in its ability to invade and host and replicate. These proteins include the F protein, nucleocapsid protein (NP), phosphoprotein (P), matrix protein (M), hemagglutinin-neuraminidase (HN) protein, and large protein. Also, more recently investigated are the W and V proteins which are thought to be encoded for by the P gene.<sup>41</sup> The F protein in accompaniment with the HN protein, form projections on the surface of the virus and attach the virion to target cell receptors. Fusion activity occurs between the virus and target cell membranes to allow for viral transcription and syncytia (giant cell) formation.<sup>37</sup>

The V protein is an interferon alpha (IFN- $\alpha$ ) and interferon beta (IFN- $\beta$ ) antagonist allowing it to provide contribution to the virus' overall virulence, by aiding its innate ability to avoid host eradication.<sup>41</sup> IFN- $\alpha$  and IFN- $\beta$  are typically produced in increased numbers by a virally-infected mammalian immune system, as these cytokines are effective at blocking viral replication.

Once cells are infected, replication of the virus occurs followed by de novo protein synthesis and caspase activation and cellular apoptosis.<sup>42</sup> Intrinsic and extrinsic pathways for apoptosis may be activated depending on the viral strain, although NDV is primarily involved in facilitation of intrinsic apoptosis, through the release of cytochrome C.<sup>43,44</sup>

*b. Use as an Oncolytic Viral Agent*

Neoplastic regression secondary to the exposure to infectious disease has been observed naturally in anecdotal medical reports in humans beginning in the late 19<sup>th</sup> century.<sup>45</sup> These observations prompted further investigation into the use of both bacteria and viruses as adjunctive cures/treatments for neoplasia. Exposure to various human disease-causing agents was subsequently associated with morbidity and/or mortality in the exposed patient, leading to the investigation of non-human specific disease agents, one of which has been NDV.<sup>46</sup>

Given the predilection of NDV to induce apoptotic cell-death following host cell replication, genetic modification of this virus has been utilized in order to encourage tumor cell-specific targeting as a method for tumor control/treatment. Additionally, NDV has been shown to have few harmful effects in exposed humans, aside from flu-like symptoms and mild conjunctivitis.<sup>47</sup> Given its species specificity, the virus has thus far not shown any evidence of

significant spontaneous mutation when used on non-species specific patients, and it does not integrate into a host's deoxyribonucleic acid (DNA).<sup>48-50</sup>

Multiple NDV strains have been utilized in both human and animal studies using various modalities, as has been discussed in the Walter et. al publication. Notably, using NDV to kill human pancreatic tumor cells in vitro can be accomplished by direct injection of infectious virus, administration of a virus infected oncolysate, and/or by way of administration of an infected whole cell vaccine. Direct injection of a mesogenic or velogenic NDV strain has been shown to replicate in tumor cells which subsequently undergo apoptosis and lysis. Lentogenic NDV strains such as LaSota, were seldom used in this way because they had been considered to be non-lytic, and therefore were thought to be less likely to have direct cytolytic effects. This was based upon evidence that the lentogenic strains require activation of the F protein by trypsin-like proteases, which are normally found in the gastrointestinal tract of poultry. However, this theory has been more recently disproven.<sup>49</sup> Krishnamurthy et al (2006)<sup>51</sup> showed that LaSota (LAS) strains of NDV replicated efficiently in four tumor cell types in vitro but, rather unfortunately, did not describe the noted cytopathic effects. Dr. Subbiah Elankumaran's laboratory here at the Virginia Polytechnic Institute, also demonstrated in vitro oncolytic activity of NDV, but in canine brain tumor patient-derived cell lines (**Figure 1**).

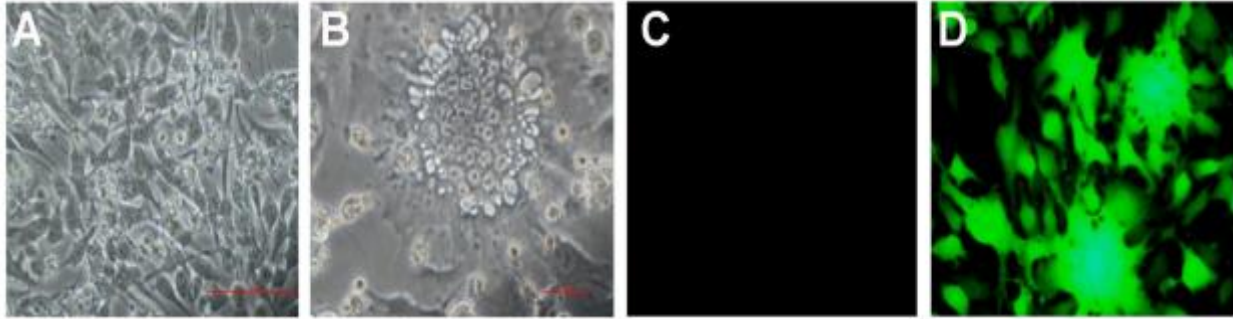


**Figure 1: Tropism modified and protease activated NDV are fusogenic in uPAR expressing canine glioma cells.** Syncytia formation in JM-877 glioblastoma cells infected with (A) PBS, (B) rLAS-uPA, (C) PBS, and (D) rLAS-uPA-eGFP

Furthermore, Elankumaran et al (2010) showed that interferon sensitive recombinant LAS NDV was effective at clearing tumor burden in experimentally induced human fibrosarcoma murine models.<sup>44</sup> Walter et al (2012) demonstrated that LAS NDV was highly cytolytic for human pancreatic carcinoma cells in vitro.<sup>48</sup>

Steiner et al (2004) also showed improvement in overall survival and disease free progression in a population of patients afflicted with glioblastoma multiforme, that were administered whole cell Ulster NDV.<sup>52</sup> Ulster is also a lentogenic form of NDV. To the author's knowledge, currently two NDV strains (MTH-68/H and HUIJ), have completed phase I clinical trials in human medicine, investigating the safety of their use in solid brain tumor treatment. The viral strains were deemed safe for systemic administration, no maximum tolerated dose was reached, and some anti-glioma cell activity was observed.<sup>53</sup> However, adjunctive treatment strategies were also employed and the studies failed to show complete resolution of tumor burden.

It is evident from the current data provided by clinical studies involving NDV as an oncolytic agent, that further investigation into the optimization of viral dose and delivery route

imperative, in order to better characterize this virus' effectiveness for treatment of solid tumors (of the nervous system, especially). Systemic administration of NDV requires the use of multiple doses in large quantities, but a dose and timeline protocol for effective treatment has not yet been clearly defined. Interestingly, there has also been shown in the current viral studies, that some patients demonstrate a low therapeutic index of NDV following systemic administration assessment. Dr. Subbiah Elankumaran's research laboratory identified that human clinical trials often report low therapeutic index of systemically administered NDV because they have been using virus that was grown in chicken eggs and is highly susceptible to the neutralizing action of human complement.<sup>54</sup> Experimental amplification of NDV in cells of homologous species allows the virus to incorporate species-specific complement inhibitors on the surface and enable the virus to evade complement.<sup>54</sup> Dr. Elankumaran's laboratory focused on the specific use of NDV as an anti-cancer agent, and developed several tropism modified recombinant NDV strains which were demonstrated to be well tolerated following systemic administration. These recombinant strains also had potent antitumor activity against a range of human and animal cancers, including brain tumors.<sup>43,44</sup>

While promising, the current data lacks substance to show that intravenous administration of any form of NDV is an effective long-term treatment option for tumors of the nervous system. It is suspected that viral-mediated oncologic targeting has shown limited effectiveness due to the inherent neutralization techniques employed by a mammalian host's immune system, and evidence for this suspicion continues to grow with further investigation.<sup>55</sup> Neutralizing antibody formulation and circulation is a strong barrier to viral oncolytic therapy, and attempts to avoid the development of this immune response include immunosuppression (using chemotherapeutic medications) and tolerization.<sup>55</sup> Tolerization involves slowly acclimating the immune system to



low level of antigen so as to avoid a potentially overwhelming immune response when the viral is finally administered.<sup>56</sup> At this time, no standardized method for evading detection by the host's immune system exists.

## 1.4 Urokinase Plasminogen Activator System

### *a. Components and Function*

The urokinase plasminogen activator (uPA) system is majorly responsible for facilitating plasminogen conversion to plasmin. Plasminogen plays a key role in the binding of fibrin and blood clot formation in most species. Plasminogen's active form, plasmin is responsible for fibrin cleavage and clot dissolution. This process occurs as a sequela to urokinase plasminogen binding to its receptor. Additionally, the uPA system is involved in other biologic processes such as matrix remodeling during wound healing, tumor invasion, angiogenesis and metastasis.<sup>57</sup>

The system is composed primarily of urokinase plasminogen activator (uPA), the receptor (uPAR), and two endogenous inhibitors (plasminogen activator inhibitor 1 and 2; PAI-1 and PAI-2). uPAR is expressed in low levels in normal tissue, and enhances the function of uPA, which has a high affinity for its receptor.<sup>58</sup>

### *b. Tumor Applications*

The system is thought to play a role in tumor formation through the following pathways: tumorigenesis, extracellular matrix degradation, cell proliferation, cell migration, cell adhesion, angiogenesis and intravasation.<sup>59</sup> Once plasminogen is converted to its enzymatically active form plasmin, it can directly activate and release growth factors found in the extracellular matrix.<sup>60</sup> This in turn, can lead to further growth factor activation and result in direct cell growth. Should

the cells affected be neoplastic in origin then this system can promote local tumor growth or distant spread.

Plasmin has also been shown in vitro and vivo to activate matrix metalloprotease precursors which can degrade the extracellular matrix and make tumor spread more efficient by encouraging vascular growth.<sup>61</sup> It has been widely documented in human patients that uPA and uPAR are highly expressed in solid tumors including those affecting mammary tissue, lung, gastrointestinal tract and the brain.<sup>60</sup> A study by Reith et al, showed that the cellular receptor for uPAR was identified in increased numbers in human glioblastoma cell lines, and it is thought that potentially the level of expression may be correlated to the malignant behavior of this tumor.<sup>62</sup> Salajegheh et al (2005) also noted that uPAR was expressed to some degree in 65 different primary brain tumors, including 5 meningiomas (Grade I).<sup>63</sup> Increased uPAR expression was noted in the astrocytoma/glioblastoma tumor subgroup, which adds further weight to this receptor's positive correlation with inherent tumor malignancy.

The expression of uPA and/or uPAR in canine brain tumors, to the author's knowledge, has not yet been described. As part of this thesis, the uPAR expression of canine tumor samples was performed and confirmed using immunohistochemistry as justification for the investigation of the development of uPA/uPAR targeted oncolytic viruses for use in dogs.

## CHAPTER 2: EXPERIMENTAL METHODS AND TRIAL PROTOCOL

### 2.1 Hypotheses and Specific Aims

**Hypothesis 1:** It was hypothesized that uPAR would be overexpressed in canine intracranial meningiomas when compared to normal brain tissues.

**Specific Aim 1.1:** To characterize the expression of uPAR in archival canine meningioma specimens and normal brain tissues using uPAR immunohistochemistry.

**Hypothesis 2:** It was hypothesized that a rLAS-uPA administered to dogs by the intravenous route (IV) would be well tolerated.

**Specific Aim 2.1 (Primary Endpoint):** To characterize the clinical, hematologic, biochemical, and neurological tolerability of escalating doses of modified recombinant Newcastle Disease virus (rLAS-uPA) that have been administered intravenously to client-owned dogs, that have been diagnosed with presumptive meningioma.

**Specific Aim 2.2:** To characterize the immune response and viral shedding and recovery in dogs treated with intravenously administered rLAS-uPA.

**Specific Aim 2.3:** To evaluate the preliminary anti-tumor efficacy of rLAS-uPA using objective tumor response criteria generated from serial magnetic resonance imaging (MRI) examinations of the brain.

## 2.2 uPAR Immunohistochemistry

Intracranial meningioma samples originated from surgical biopsy or resection specimens, necropsy samples, or archival paraffin-embedded specimens from clinical cases presented to the Veterinary Teaching Hospital of the Virginia-Maryland College of Veterinary Medicine. Five normal brain samples (meninges, cerebral cortex, and choroid plexus) were collected from necropsy and archival paraffin-embedded materials from dogs with no clinical, magnetic resonance imaging, or histopathological evidence of brain disease. Clients provided written consent for their dog's tissues to be banked and in a biospecimen repository and used for research purposes (IACUC Approval 13-153-CVM). All tumors were classified and graded by veterinary pathologists according to World Health Organization criteria by examination of hematoxylin and eosin (H&E), vimentin stained slides prepared from formalin-fixed, paraffin-embedded specimens, as previously reported.<sup>64</sup>

Five  $\mu\text{m}$  sections were cut from each paraffin embedded block, mounted on positively charged slides, placed in a drying oven at 40°C for 30 minutes and then placed in a drying oven at 65°C for 30 minutes. Immunohistochemistry was performed using a procedure modified from a previously described protocol using an automated staining system (BenchMark XT, Ventana Medical Systems Inc., Tucson, AZ, USA) and an alkaline phosphatase detection method (Enhanced Alkaline Phosphatase Detection Red Kit, Ventana).<sup>65</sup> Epitope retrieval was performed with Cell Conditioning 1 Solution (Ventana) at 96°C for 90 minutes, followed by rinsing in Reaction Buffer (Ventana). Following rinsing, slides were incubated with a murine anti-uPAR antibody (M7294, Clone, DAKO, Santa Cruz, CA, USA; 1:25 dilution using Antibody Dilution Buffer (Ventana) at 37° for 2 hours, and then rinsed three times for 2 minutes each with Reaction

Buffer. Slides were subjected to automated amplification (Amplification Kit, Ventana) for 16 minutes and endogenous biotin blocking (Blocking Kit, Ventana) for 8 minutes prior to the additional of the secondary biotinylated goat anti-mouse/anti-rabbit antibody for 30 minutes, and rinsed with Reaction Buffer. Slides were incubated with a streptavidin-alkaline phosphatase conjugate in Tris buffer with MgCl<sub>2</sub> and ZnCl (Ventana) for 30 minutes. Slides were then developed with a naphthol substrate and fast-red chromogen (Ventana, Fast Red) for 15 minutes, counterstained with Richard-Allan Hematoxylin, and dried at room temperature. Negative controls were performed by substituting the primary antibody with Antibody Dilution Buffer (Ventana). Canine tonsils and intestines were used as the positive control tissue.<sup>65</sup>

### **2.3 Canine Trial Eligibility Criteria and Recruitment**

The study protocol was approved by the Virginia Tech (VT) Institutional Animal Care and Use Committee 15-013-CVM), the VT Institutional Biosafety Committee (IBC#12-041), and the Veterinary Teaching Hospital Review Board. Canine patients were required to have a diagnostic brain MRI prior to enrollment demonstrating an extra-axial mass lesion with imaging characteristics consistent with a meningioma.<sup>13</sup> All masses were required to measure at least 10 mm in diameter, in a single plane based upon assessment of T1-weighted post-contrast images. This requirement was adopted in cooperation with the Response Assessment in Veterinary Neurooncology (RAVNO) criteria for inclusion of patients with measurable disease.<sup>66</sup>

No exclusion parameters were placed on patient signalment. Additionally, the pursuit of alternative therapeutic options such as cytoreduction, biopsy, and/or radiation therapy, did not immediately result in exclusion, but was required to have occurred at least 4 weeks (surgery) or 4

months (radiation therapy) prior to enrollment. Further eligibility was set for as possessing a Karnofsky performance score (KPS) of at least 50, having stable cardiopulmonary functions, receiving (if applicable), a stable or decreasing dose of corticosteroids, and medically controlled seizures.

Hepatic, renal, and bone marrow functional requirements were as follows: liver function tests  $\leq 3$  times of the high-end of normal canine references ranges, creatinine  $\leq 1.8$  mg/dl, hematocrit  $\geq 33\%$ , segmented neutrophils  $\geq 1,500/\text{mm}^3$ , and platelet count  $>100,000/\text{mm}^3$ . Patients were excluded from the trial if they were immunocompromised, pregnant, lactating, or receiving any other anti-cancer treatment during the study period. Pet-owners were required to sign a written informed consent document approved by IACUC and the Veterinary Teaching Hospital Review Board in order to enroll their dogs in the study.

Timely patient recruitment for this trial was facilitated through dissemination of a non-technical written and web-based summaries of the study to the public and veterinary health care professionals by way of the infrastructure provided by the Veterinary Clinical Research Office, in conjunction with our veterinary specialist research partners in the regional Collaborative Research Network. Funding for the trial was obtained from the Virginia Veterinary Medical Association Pet Memorial Fund and NIH NIAID R21AI070528. The trial duration was 42 days, and clinical workflow is summarized in **Table 3**.

#### **2.4 Assessment of Safety and Tolerability (Primary Endpoint)**

Safety was assessed by clinical and laboratory evaluations of each canine patient performed every 14 days for 6 weeks. Each visit included physical and neurological examinations,

monitoring and recording of vital parameters during treatment (rectal temperature, heart rate, respiratory rate, and body weight) and serial laboratory profiling, consisting of a CBC, serum biochemistry profile, and urine analysis. Adverse events were classified, graded, and recorded according to Veterinary Cooperative Oncology Group and National Cancer Institute Common Terminology Criteria for Adverse Events metrics.<sup>1</sup> Safety was defined by the absence of any study-related grade 3 (severe), 4 (life-threatening), or 5 (fatal) adverse events. Dose limiting toxicity was defined as the presence of any study-related grade 3, 4, or 5 adverse event. Clear exacerbation or progression of pre-existing tumor-associated clinical signs were not considered to be dose limiting. As fever is one of the most commonly reported adverse events associated with rNDV therapies, the pet-owners were also instructed and trained to check and record their dog’s rectal temperature daily during the study on record these findings on a study calendar.

**Table 3: Canine rLAS-uPA Clinical Trial Workflow**

Monitoring	Methods	Time Point (Days)				
		<0	1	14	28	42
Clinical Signs, Rectal Temperature, Adverse Events	Owner + DVM	Daily →				
Laboratory						
• CBC, Serum Biochemistry, UA		X	X	X	X	X
• Cerebrospinal fluid		X/-				X
Immune Response						
Serum						
• Anti-NDV antibodies	PNA		X	X	X	X
• TNF- $\alpha$ , IFN- $\gamma$ , TRAIL	ELISA		X	X	X	X
Viral Shedding						
• Blood	IVR		X	X	X	X
• Cerebrospinal fluid	IVR					X
• Urine	IVR		X	X	X	X
Tumor Response	Brain MRI	X				X
<b>Intervention</b>						
rLAS-uPA IV Infusion						

**Table 3 Key Abbreviations:** ELISA= Enzyme linked immunoassay; IVR= Infectious viral recovery; PNA= Plaque neutralization assay

## 2.5 Formulation and Dosing of rLAS-uPA for Clinical Use

### *a. rLAS-uPA Newcastle Disease Viral Formulation- Cells and Virus*

Human epithelial carcinoma cells (HeLa CCL2; ATCC, Manassas, VA, USA) were grown and maintained in Dulbecco Modified Eagle Medium (DMEM) supplemented with 10% heat-inactivated fetal bovine serum (FBS), 100  $\mu$ g of penicillin/mL, and 0.1  $\mu$ g of streptomycin/ml (Invitrogen, Carlsbad, CA, USA), in a 5% CO<sub>2</sub> incubator at 37° Celsius (C). The full-length infectious clone of NDV strain LaSota was a gift from Dr. Siba K. Samal, University of Maryland, College Park, MD, USA. The native LaSota strain was genetically modified as previously described such that the LaSota fusion (F) protein cleavage site was replaced with uPA cleavage site, generating the recombinant strain rLAS-uPA.<sup>43,44</sup> All experiments involving NDV were performed in our Biosafety Level-2 or Biosafety Level-3 facilities following the guidelines and approval of the Virginia Tech Institutional Animal Care and Use (Protocol 15-013-CVM) and Biosafety Committees (Protocol 12-041).

### *b. rLAS-uPA Newcastle Disease Viral Formulation- Viral Propagation*

The rLAS-uPA viral stock was serially diluted ten-fold to a 10<sup>-3</sup> dilution in plain DMEM and kept on ice. HeLa cells were propagated to a monolayer in T-150 cm<sup>2</sup> tissue culture flasks in DMEM+10% FBS+100  $\mu$ g of penicillin/mL, and 0.1  $\mu$ g of streptomycin. Spent media from the tissue culture flasks containing HeLa cell monolayer was discarded and the cells are washed once with 10 mL of phosphate buffered saline (PBS). Following washing of the HeLa monolayer, 6 mL of the 10<sup>-3</sup> virus dilution was added to the tissue culture flasks and the cells incubated in CO<sub>2</sub> for 2 hours at 37°C with gentle rotary shaking performed every 15 minutes.



After the 2-hour incubation, the viral inoculum was removed and discarded, and the cells in each flask supplemented with 30 mL DMEM with 0.5µg urokinase plasminogen activator (uPA, recombinant human, Ray BioTech, GA, USA). Cells were then incubated in CO<sub>2</sub> for 5 days at 37C, and the cells monitored daily for cytopathic effect (CPE). When the cells attained 80% CPE, the tissue culture flasks were frozen at -80°C.

*c. rLAS-uPA Newcastle Disease Viral Formulation- Viral Purification*

Frozen tissue flasks were thawed in a room temperature water bath, and the contents transferred to 50 mL conical tubes and clarified by centrifugation at 4000 revolutions per minute (rpm) for 15 minutes at 4°C in a swing rotor. The clarified tissue-culture-fluid containing virus was then aliquoted and subjected to purification by ultra-centrifugation.

Aliquots of tissue culture fluid containing virus were overlaid over a 10-mL cushion of 20% sucrose solution in ultra-thin centrifuge tubes (344058, Beckman Coulter, Brea, CA, USA) and the contents centrifuged at 25,000 rpm for 2 hours at 4°C using tan SW28 rotor (Bekman Coulter). Following centrifugation, the supernatant is siphoned and discarded, leaving the viral pellet. The pellet is suspended in 1mL PBS with Ca<sup>2+</sup> and Mg<sup>2+</sup> and the tube stored at 4°C overnight.

In an ultra-thin centrifuge tube fitted for an SW41 rotor (344059, Beckman Coulter), 5 mL of 20% sucrose solution is overlaid upon of 5 mL of 60% sucrose solution to obtain a discontinuous sucrose gradient, upon which 1.5 ml of the re-suspended viral pellet was overlaid. The tube contents were then contents centrifuged at 25,000 rpm for 2 hours at 4C using tan SW41 rotor (Bekman Coulter). Following centrifugation, the virus settles in-between the sucrose gradient layers, appearing a hazy white solution. Three mL of this hazy white solution

was collected, diluted in 30 mL of ice-cold of PBS with  $\text{Ca}^{2+}$  and  $\text{Mg}^{2+}$  and then ultra-centrifuged at 25,000 rpm for 2 hours at 4°C using tan SW28 rotor. The supernatant was then discarded, 1 mL PBS added to the pellet, and the tubes stored at 4°C overnight. After overnight incubation at 4°C, the ultra-purified virus pellet was re-suspended, aliquoted, and stored at -80°C for future use.

#### *d. Plaque Assay and Viral Dosing*

Quantification of the number of infectious units in viral suspensions dosed to canine patients was performed using standard plaque assay. Briefly, twelve well tissue culture plates were seeded with  $0.3 \times 10^6$  cells/mL of DF-1 fibroblast cells (ATCC) or in DMEM with 10% fetal bovine serum (FBS), and assay performed on the day monolayers reached confluence. A methylcellulose overlay medium was prepared by placing 4g methylcellulose (M0512, Sigma, S. Louis, MO, USA) into a medium glass flask. A magnetic stir bar was added to the flask and the contents autoclaved. Following cooling to room temperature, 500 mL of DMEM was added to the sterile methylcellulose and the mixture stirred for 24 hours.

Serial tenfold dilutions ( $10^{-1}$  to  $10^{-9}$ ) of rLAS-uPA were prepared in DMEM with 0.5 with 0.5µg uPA. Excess media from the tissue culture monolayers of DF-1 cells was discarded, and 0.1 mL of virus dilution was added to each of the duplicate tissue culture monolayers. The plates were rocked gently to achieve an even distribution of the virus. The virus was allowed to adsorb for 60 minutes at 37°C in a CO<sub>2</sub> incubator, and the plates gently and manually tilted every 15 minutes to avoid drying of the cell monolayers. The unabsorbed virus was removed and the cells were washed once with PBS. One mL of the methylcellulose overlay was added to each of

the 12 wells of the tissue culture plate, and the plate allowed to incubate for 96 hours at 37°C in a CO<sub>2</sub> incubator. Following removal of the plated from the incubator, the methylcellulose overlays were removed and discarded. Cells in the plates were fixed and stained with 1% crystal violet solution prepared in 10% buffered formalin phosphate (0.5 mL/well) for 90 minutes at room temperature. Excess stain was drained, the plated washed with distilled water and allowed to air dry. Plaques were counted using a stereomicroscope, and the infectivity titer expressed as the number of plaque forming units per mL, obtained using the following formula:

**Formula 1.1** Plaque number x reciprocal of dilution x reciprocal of inoculum volume in mL.

The trial followed a conventional 3+3 dose-escalation design with predetermined dosing cohorts. The rLAS-uPA dosing cohorts used in this study are summarized in **Figure 2**, and the dose escalation criteria and dose-limiting toxicities summarized in **Table 4**. The starting dose was based upon the median tissue culture infective dose (TCID<sub>50</sub>) obtained from J3T canine glioma cell line experiments performed in Dr. Subbiah Elankumaran's laboratory (data not shown). Prior to administration to canine enrollees, the virus formulation was thawed, sonicated briefly and diluted to provide the required dose. All doses were then administered as a slow intravenous infusion in sterile physiological (0.9%) sterile saline over a period of 2 hours. Each dog enrolled at each dose level received 3 intravenous doses of virus infusate administered 14 days apart (**Figure 2**).

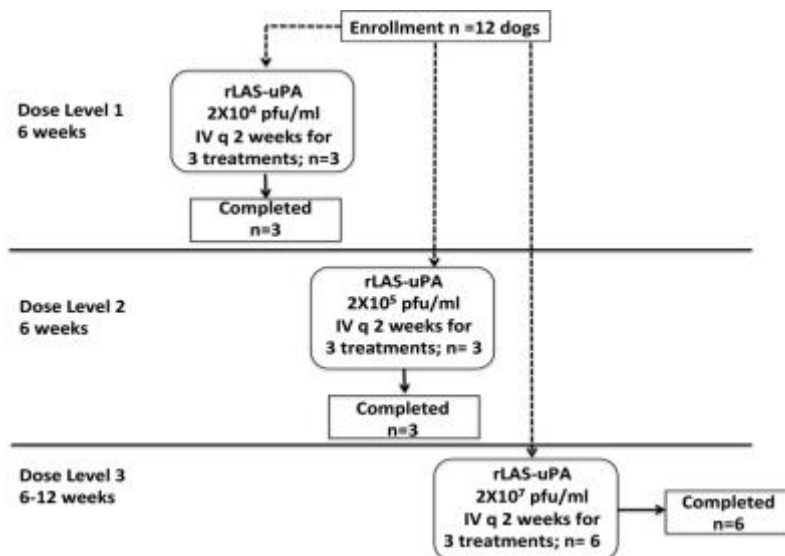


**Figure 2: rLAS-uPA Dosing Cohorts and Schema**

**Table 4: Phase I, 3+3 Conventional Dose Cohort Escalation Decision Design**

Number of Patients with Dose Limiting Toxicity (DLT) at Dose Level	Dose Escalation Decision Rule
0 out of 3	Enter 3 patients at next dose level
$\geq 2$	Dose escalation is stopped <ul style="list-style-type: none"> <li>This dose declared maximum administered dose (MAD);</li> <li>3 more patients entered at next lowest dose level if only 3 patients previously treated at that dose</li> </ul>
1 out of 3	Enter 3 more patients at this dose level <ul style="list-style-type: none"> <li>If none of these patients experience DLT*, then escalate to next dose level</li> <li>If 1 of these patients experiences DLT then dose escalation is stopped and this dose declared MAD</li> <li>3 more patients entered at next lowest dose level if only 3 patients previously treated at that dose</li> </ul>
$\leq 1$ out of 6 at highest dose level below MAD	This is considered the maximal tolerated dose (MTD) and generally recommended for Phase II testing. At least 6 patients must be entered at the recommended Phase II dose.

\* DLT defined as a study-related grade 3 (severe), 4 (life-threatening), or 5 (fatal) AE.<sup>25</sup>

Each infusion was administered on an out-patient basis, with discharge into the pet-owners care after approximately four hours post-infusion. Daily rectal temperature readings were instructed to be taken during the study in order to monitor for the development of fever.

## **2.6 Canine Biological Sample Collection**

The frequency with which the following biological samples were obtained from each patient in the clinical trial is provided in **Table 3**.

### *a. Blood*

Blood samples were collected via jugular or saphenous venipuncture into Vacutainer PST, serum, K2EDTA (Becton-Dickinson, New Jersey, USA) tubes for performance of the CBC and serum biochemical analyses. A 1mL aliquot of whole blood from K2EDTA was then transferred to RNeasy protect animal blood tubes (Qiagen, CA, USA), for future preservation for isolation of RNA. An additional 2 mL aliquot of serum was harvested and frozen at -80C for future immunological assays.

### *b. Urine*

Urine was obtained using cystocentesis and free-catch techniques. Freely caught urine was collected into clean plastic specimen receptacles. Urine samples were aliquoted into 8 ml sterile falcon tubes (Becton-Dickinson), centrifuged at 1000 g for 10 minutes at 4°C, and the urine pellet collected and suspended in 1 ml Qiazol (Qiagen). Urine samples were stored -80°C.

### *c. Cerebrospinal Fluid*

While under general anesthesia and following completion of brain MRI procedures, cerebrospinal fluid was collected from the cerebellomedullary cistern using routine methods.<sup>67</sup>

## **2.7 Canine Immune Responses to rLAS-uPA**

### *a. Infectious Viral Recovery (IVR)*

Viral recovery was performed in accordance with the international trade standards as described by the World Organization of Animal Health.<sup>89</sup> Sample supernatants (whole blood or urine) were obtained through clarification by centrifugation at 1000 g for 10 minutes at 15°C. Aliquots of 0.2 mL of supernatant were inoculated into the allantoic cavity of each of at five embryonated SPF chicken eggs (Charles River Laboratories, CT, USA) of 9-11 days incubation.

Following inoculation, eggs were incubated at 37°C for 4-7 days. Checks for bacterial contamination were performed by streaking samples in Luria Broth agar plates and reading these at 24 and 48 hours of incubation against a light source. Contaminated samples were treated by incubation with increased antibiotic concentrations for 2–4 hours (gentamicin, penicillin g, and amphotericin b solutions at final concentrations to a maximum of 1 mg/mL, 10,000 U/mL, and 20 µg/ml, respectively). To accelerate the final isolation, two passages were performed at the 3-day interval, obtaining results comparable to two passages at 4–7-day intervals. Eggs containing dead or dying embryos as they arise, and all eggs remaining at the end of the incubation period, were chilled to 4°C for 4 hours or overnight and the allantoic fluids tested for hemagglutination (HA) activity. Fluids that yielded a negative reaction were passed into two further batch of eggs.

*b. Anti-rLAS-uPA Antibodies*

The antibody levels of serum samples collected from dogs treated with rLAS-uPA were evaluated by hemagglutination inhibition (HI) and virus neutralization (VN) assays.

***i. Hemagglutination Inhibition (HI) Assay***

A day prior to HI assay, serum samples from dogs treated with rLAS-uPA, control dogs, and NDV immunized chickens were exposed to with RDE-II (receptor-destroying enzyme II, YCC340122, Accurate Chemical and Scientific Corporation, USA) to remove non-specific hemagglutination. RDE-II treatment was performed by adding 50µl of serum to 200µl RDE-II (1:10 dilution in calcium saline solution equaling 100 units per ml) and incubated overnight in a 37°C water bath. Next, 150µl of 2.5% sodium citrate solution was added and then heat inactivate at 56°C for 30 minutes. Finally, 100µL of PBS was added to obtain a 1/10 dilution of the serum.

Test groups for the HI were as follows: 1) rLAS-uPA + NDV treated canine sera (test); 2) rLAS-uPA + Untreated canine sera (negative canine control); 3) rLAS-uPA + NDV immunized chicken sera (positive control); 4) rLAS-uPA + PBS (virus control); and 5) PBS + PBS (uninfected control).

A rLAS-uPA viral dilution was prepared to 8HA unit/25µL in sterile PBS. In a 96-well V-bottom plate, 50µL of RDE-II treated test sera from each test group was added to the first well of rows A-F of the 96 well plate. The serum samples were serially diluted (2-fold dilutions in PBS) in 25µL volumes in the remaining wells in each row (i.e. through column 12) of the plate. In the first wells of rows G and H plain PBS was included for the virus and uninfected controls.

Next, 25µL of purified rLAS-uPA virus dilution (i.e. 8 HA unit) was added to 25µL of various dilutions of sera samples or PBS, and incubated at room temperature for 1 hour. The virus was not added to uninfected control wells (PBS+PBS). After 1 hour of incubation, 50µL of 0.5% chicken RBC suspension (Alsevers Chicken Blood, Lampire Biologicals Laboratories, PA, USA) was added to all wells and the plates placed on a rotary agitator to mix thoroughly.

The plates were covered with sealing tape and incubated at room temperature until a distinct button formed in the positive control wells. The plates were examined after about 20 minutes incubation for evidence of hemagglutination. Serum samples were considered positive for the specific virus if hemagglutination is inhibited. The test was considered valid if the positive control (i.e. virus + positive chicken sera) demonstrated the expected HI titer and the back titration of virus is 8 HA units. The endpoint of the titration was considered the reciprocal of the highest dilution of the serum causing complete inhibition of hemagglutination. Any HI titers below the limits of detection (i.e. 20) were denoted as half of the threshold detection value (i.e. 10).

#### *ii. Virus Neutralization (VN) Test*

The virus neutralization test was carried out using pre- and post-treatment canine sera in DF1 cells grown in 96-well tissue culture plates according to standard methods.<sup>55</sup> Briefly, 2-fold serial dilutions of 50-µL serum samples (complement inactivated) were carried out and incubated for 1 hour with 100 TCID<sub>50</sub> of rLAS-uPA in DMEM. Following incubation, cells were infected with virus-serum mixture. The VN titer was obtained by confirmation of the presence of virus in wells with the highest dilution of serum.



*c. Canine Cytokine ELISA Assays*

To evaluate canine immune responses to the rLAS-uPA, ELISA assays were performed to quantify serum concentration of tumor necrosis factor alpha (TNF- $\alpha$ ), interferon gamma (IFN- $\gamma$ ), and tumor necrosis factor related apoptosis inducing ligand (TRAIL).

The TNF- $\alpha$  ELISA was performed using a commercially available canine specific kit (Canine TNF- $\alpha$  Quantikine ELISA, R&D Systems, Minneapolis, MN). Assays were performed in duplicate using 100 $\mu$ l aliquots of pre- and post-immune canine sera serially diluted (1:10-1:100,000) in antibody-conjugate diluent according to the manufacturer's instructions. Microplates were and read at 450 nm using a spectrophotometer (Spectramax Plus 384, Molecular Devices, CA, USA). This kit has reported inter- and intra-assay coefficients of variation of 8% and 9%, a detection sensitivity of 4.2 pg/mL.

The IFN- $\gamma$  ELISA was performed using a commercially available canine specific kit (Canine IFN- $\gamma$  Quantikine ELISA, R&D Systems, Minneapolis, MN). Assays were performed in duplicate using 100 $\mu$ l aliquots of pre- and post-immune canine sera serially diluted (1:10-1:100,000) in antibody-conjugate diluent according to the manufacturer's instructions. Microplates were and read at 450 nm using a spectrophotometer (Spectramax Plus 384, Molecular Devices, CA, USA). This kit has reported inter- and intra-assay coefficients of variation of 8% and 5%, a detection sensitivity of 60 pg/mL.

The TRAIL ELISA was performed using a commercially available kit specific for detection of the canine ligand (Dog TRAIL, #abx150298, Abxexa Ltd. Cambridge, UK). Assays were performed in duplicate using 100 $\mu$ l aliquots of pre- and post-immune canine sera serially diluted (1:10-1:100,000) in antibody-conjugate diluent according to the manufacturer's instructions. Microplates were and read at 450 nm using a spectrophotometer (Spectramax Plus

384, Molecular Devices, CA, USA). This kit has reported inter- and intra-assay coefficients of variation of 7% and 6%, a detection sensitivity of 0.06 ng/mL.

Effects of treatment and time on each measured quantitative ELISA variable in the dogs were assessed by use of repeated measures ANCOVA. The linear model included the baseline measurements as a covariate. Significance was set at  $\alpha = 0.05$ . All analyses were performed with a statistical software package (SAS, version 9.1.3, SAS Institute Inc., Cary, NC, USA).

## 2.8 Assessment of Therapeutic Response to rLAS-uPA

### *a. Response Assessment (MRI-Based) Evaluation of Tumors*

Magnetic Resonance Imaging (MRI) examinations of the brain were performed under general anesthesia approximately six weeks following initiation of the viral treatment in all enrollees. Additionally, 1 dog was randomly selected for an additional follow-up MRI examination approximately 3 months following trial enrollment. Follow-up MRI examinations were reviewed and qualitative and quantitative assessments of tumor response were determined using the following Response Assessment in Veterinary Neurooncology (RAVNO) criteria as published by Rossmeisl et al.<sup>66</sup>

- Partial Response (PR):  $\geq 50\%$  reduction in the enhancing tumor sum products of diameters
- Stable Disease (SD):  $< 50\%$  decrease or  $< 25\%$  increase in contrast enhancing tumor sum products of diameters

- Progressive Disease (PD): >25% increase in contrast enhancing tumor sum products of diameters.

Each set of images was reviewed and assessed by a board-certified radiologist, board-certified neurologist, and neurology resident. All post-treatment brain MRI images were obtained routinely under general anesthesia using a 1.5 Tesla magnet (Philips Intera, Andover, MA, USA). Standard images were acquired in the transverse, sagittal and dorsal planes using T2W, FLAIR, FFE (GRE), and T1W pre-and-post gadolinium-based contrast agent administration (Magnevist, Bayer, Whippany, NJ, USA) sequences. Following image acquisition, each data set was analyzed for target (contrast enhancing) and non-target (non-contrast enhancing) lesions using standard viewing software such as eFilm (Merge, IBM, Chicago, IL, USA) and/or Horos (The Horos Project, version 2.0). The lesions were compared to pre-enrollment imaging provided by referral institutions and/or the VMCVM VTH similarly to above. Quantitative assessment of the lesions was obtained through target lesion diameter measurement following RAVNO guidelines, in the transverse, dorsal and sagittal planes. The measurements were assessed individually by each observer and the longest diameter as well as a corresponding perpendicular measurement were calculated and recorded. The largest diameters between pre-and post-treatment images were compared in order to provide a subjective assessment of tumor behavior (progression, stable, reduction).

#### *b. Time to Progression*

Surrogates of progression included deterioration in Karnofsky performance score from baseline, development of new or progression of pre-existing tumor-associated neurological deficits, objective tumor progression as determined from RAVNO MRI assessments, and/or

death. Progression free survival (PFS) was determined from the day of study enrollment until the day of documented death, if applicable.

*c. Identification of rLAS-uPA in Canine Tissues by RT-PCR*

Tumor samples were collected and stored frozen at -80°C from any patient enrolled in the study who underwent surgical resection of the tumor following completion of the study, or who died or was euthanized during the course of the study, and whose owners consent to performance of a necropsy examination. mRNA from canine tumors and blood was isolated using an RNeasy kit (Qiagen, Valencia, CA, USA) according to the manufacturer's instructions.

A seminested RT-PCR for rLAS-uPA was performed using previously described methods (Seal). The primers used for RT-PCR were generated by alignment of published NDV nucleotide sequences (Genebank, representing a segment of the open reading frame for the matrix gene. The outer set of primers were as follows: M0 (sense), 5'-GAGTTACTTTCYKCTGCRATGCTCTGCCTAGG-3'; M2 (antisense), 5'-GTCCGAGCACATTGAGC-3'. The seminested primers were M1 (sense), 5'-TCGA-GICTGT AIAATCTTGC-3' and M2 (antisense), which generates a 232 bp amplicon. These primer sequences are known to be useful in the characterization of a large number of NDV pathotypes (Seal BS reference). For reverse transcription, 1 mg of extracted nucleic acid was added to the following reaction mix: 1 mL of oligo (dT) 12–18 (500 mg/mL), 1 mL of 10 mM dNTP mix (Invitrogen, Carlsbad, CA, USA) and nuclease-free water to a total reaction volume of 17 mL. As positive control, 1 mL of rLAS-uPA nucleic acid was collected from amniotic fluid of an infected embryonated egg. For a negative control, nuclease-free water was added instead of sample nucleic acid. The reaction was incubated in a 65°C bath for 5 minutes and then placed on ice for 2 minutes. The contents were collected by

brief centrifugation and mixed with 4  $\mu$ l of 5x first-strand buffer (Invitrogen) 2  $\mu$ l of 0.1 M dithiothreitol (DTT) 1  $\mu$ l of RNaseOUT recombinant ribonuclease (Invitrogen) and 1  $\mu$ l of SuperScript II RNase H2 Reverse Transcriptase (Invitrogen). The reaction was incubated in a 50°C bath for 1 hour and then inactivated by heating at 70°C for 15 minutes.

The PCR was performed in a 50- $\mu$ l volume containing 3  $\mu$ l of sample cDNA, 25  $\mu$ l of TaqPCR Master Mix (Qiagen), 0.5  $\mu$ l of each primer (M0 and M2), and 21  $\mu$ l of nuclease-free water. The reaction was then incubated in a thermo-cycler under the following conditions: 94°C for 5 minutes; 35 cycles of 94°C for 30 seconds (denaturation), 55°C for 30 seconds (annealing), and 72°C for 1 minute (extension). The samples were then chilled at 4°C. For the second round of PCR, 3  $\mu$ l of the first PCR product was amplified by using the same reaction conditions used for the first PCR, with the primers M1 and M2. A total of 5  $\mu$ l of each seminested PCR product was subjected to agarose gel electrophoresis on a 2.0% agarose gel in TAE buffer (40- mM Tris-acetate, 2-mM ethylene-diaminetetraacetic acid [EDTA]) for 45 minutes at 90 V.

## CHAPTER 3: RESULTS

### 3.1 uPAR Immunohistochemistry

A total of 21 canine intracranial meningioma samples were included in analyses of uPAR immunohistochemical expression. Of the meningiomas samples examined, 14/21 were WHO Grade I tumors, and 7/21 were WHO Grade II tumors.<sup>30</sup> Five normal brain samples (meninges, cerebral cortex, and choroid plexus) were collected from necropsy and archival paraffin-embedded materials from dogs with no clinical, magnetic resonance imaging, or histopathological evidence of brain disease. Clinicopathologic data for individual patient samples can be found in Rossmeisl et al 2017.<sup>64</sup>

In normal brain tissue controls, uPAR immunoreactivity was observed in rare microglia and vascular endothelium contained within the cerebral cortex, as well as consistently in the choroid plexus vascular endothelium. No uPAR immunoreactivity was observed in normal meninges. In total, 19/21 meningiomas demonstrated immunoreactivity to uPAR, including 12/14 Grade I tumors and 7/7 Grade II tumors (**Figure 3**). In 6/14 Grade I meningiomas, uPAR immunoreactivity was predominantly localized to the endothelial cytoplasm within the tumor vasculature (**Figure 3A and B**), with < 5% of neoplastic cells demonstrating uPAR immunoreactivity in these cases. In 6/14 Grade I and 7/7 Grade II meningiomas mildly to markedly intense cytoplasmic immunoreactivity was observed in tumor, stromal, and vascular endothelial cells (**Figure 3C-D**). In Grade I meningiomas, uPAR immunoreactivity in these tumor cellular populations was mild and multifocal in 4/6 cases, whereas in Grade II meningiomas uPAR immunoreactivity was intense and diffuse in 4/7 cases.

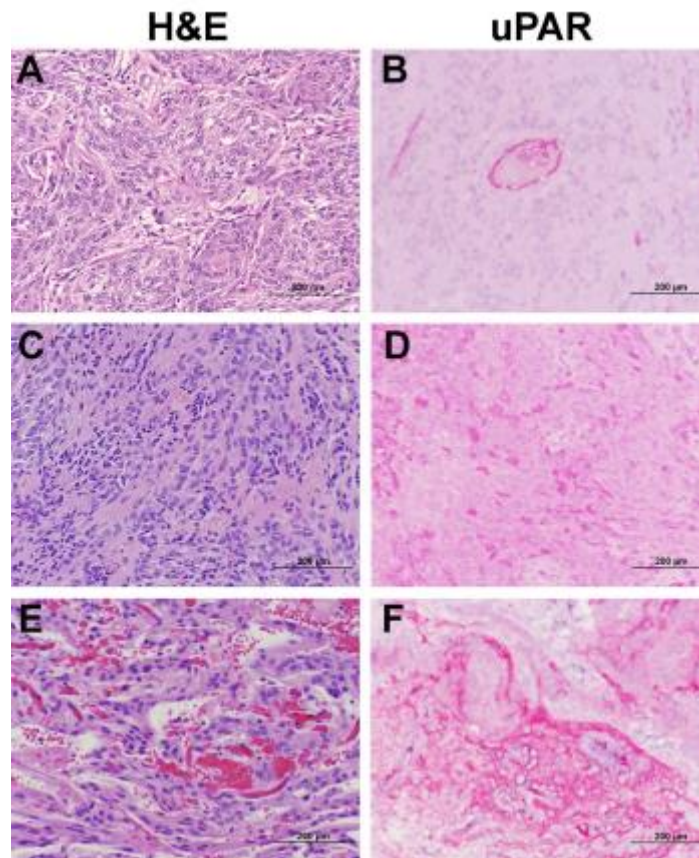


**Figure 3: uPAR immunoreactivity in canine meningiomas.**

Grade I transitional meningioma (A, H&E stain) demonstrating uPAR immunoreactivity (B) that is restricted to the endothelium of the tumor vasculature. Grade II meningioma (C, H&E stain) and angiomatous meningioma (E, H&E stain) both demonstrating immunoreactivity to uPAR in tumor cells, tumor vascular endothelium, and fibrovascular stromal cells (D, F).

Panels E and F from Patient C.

## 2.3 Phase I Clinical Trial

### *a. Canine Patients Enrolled*

Four client owned dogs (Patients A-D met the inclusion criteria for enrollment in the clinical trial (**Table 5**). All of the dogs successfully completed the clinical trial. Enrollment and treatment was performed from June 2015 to February 2016. The median age of the dogs enrolled in trial was 10 years, which corroborates the current published data on age at diagnosis of meningiomas in veterinary medicine.<sup>17</sup> Only a single dog had documented histopathologic confirmation of a Grade I angiomatous meningioma (Patient C, **Table 5**). The remaining 3 dogs had presumptive diagnosis of meningioma based upon MRI characteristics. The trial was prematurely closed in February of 2016 due to an interruption in the supply of the clinical grade rLAS-uPA due to unforeseen circumstances.

### *b. rLAS-uPA Dosing and Assessment of Safety and Tolerability*

Patients A-C (**Table 5**) received the initial dosing level of rLAS-uPA of  $2 \times 10^4$  PFU. Dog D received the second dose level of rLAS-uPA ( $2 \times 10^5$  PFU). No dose limiting toxicities were observed during the infusion period in any dog, although all animals (patients A-D) were observed shivering intermittently during infusions (**Table 6**). The shivering did not persist during the entire infusion, nor post-administration. No possible signs of anaphylactoid reaction (i.e. urticaria, vomiting, edema) were noted in any dog at any time over the course of the infusion.



**Table 5: Canine Meningioma Patient Demographics**

<b>Patient</b>	<b>Signalment</b>	<b>Clinical Signs</b>	<b>Tumor Location</b>	<b>Diagnosis</b>	<b>Admission KPS</b>	<b>Prior Therapy</b>
<b>A</b>	11 YO FS Labrador/Shepherd	Seizures	Right Parasagittal Frontal-Parietal Lobes	Presumptive MRI	75	Steroid
<b>B</b>	12 YO FS Eskimo Spitz	Seizures	Left Cystic Olfactory Bulb	Presumptive MRI	95	AED Steroid
<b>C</b>	5 YO MC Pomeranian /Terrier	Seizures	Right Cerebral Convexity Temporal-Occipital Lobes	Biopsy: Angiomatous meningioma	95	Surgery AED Steroid
<b>D</b>	8 YO MC Jack Russell Terrier	Chiasmal Blindness	Suprasellar Olfactory-Frontal Lobes	Presumptive MRI	90	None

**Table 5 Abbreviation Key:** AED= anti-epileptic drug; FS= female spayed; KPS= Karnofsky

Performance Score; MC = male castrated; MRI= magnetic resonance imaging; YO = years old.

**Table 6: Adverse Events (AE) Observed During Trial**

<b>Patient</b>	<b>Infusion AE</b>	<b>AE SOC/ Grade</b>	<b>Attribution</b>	<b>Post-Infusion AE</b>	<b>AE SOC/ Grade</b>	<b>Attribution</b>
<b>A</b>	Shivering	Administration Reaction Grade 1	Probable/Definite	Seizures	Nervous Grade 1	Unlikely
				Status Epilepticus	Nervous Grade 4	Possible
				Fever	Constitutional Grade 2	Possible
				Diarrhea	Gastrointestinal Grade 2	Unlikely
				Cystitis	Renal/Urogenital Grade 2	Unrelated
				Cardiopulmonary Arrest	Cardiac/General Grade 5	Possible
<b>B</b>	Shivering	Administration Reaction Grade 1	Probable/Definite	Diarrhea	Gastrointestinal Grade 1	Unlikely/Possible
				Seizures	Nervous Grade 1	Unlikely/Possible
<b>C</b>	Shivering	Administration Reaction Grade 1	Probable/Definite	Seizures	Nervous Grade 1	Unlikely/Possible
<b>D</b>	Shivering	Administration Reaction Grade 1	Probable/Definite	None	Not Applicable	Not Applicable

**Table 5 Abbreviation Key:** SOC= System/organ classification

In post-infusion periods, three dogs (patients A-C) experienced seizures. This progressed to status epilepticus (SE), less than 12 hours following completion of the third infusion in patient A. The severity of neurological deterioration following the onset of the status epilepticus in patient A ultimately resulted in owner-requested euthanasia.

There were no significant hematologic or biochemical toxicities observed in the trial in any dog (data not shown). Asymptomatic Grade 1 hematological and biochemical adverse events, such as elevations in hepatic ALP and ALT enzymes were observed in all dogs, but were attributed exclusively to concurrent medications with AED and corticosteroids. Post-treatment cerebrospinal fluid (CSF) analyses were grossly, biochemically and cytologically unremarkable in patients A, B, and D. In patient C, post-treatment CSF analysis revealed a moderate lymphocytic pleocytosis (total nucleated cell count of 86/ $\mu$ L [reference range < 3  $\mu$ L] and total protein of 20.9 mg/dL [reference range < 25 mg/dL]).

*c. Canine Immune Responses to rLAS-uPA*

No infectious virus was recovered from any dog's blood, urine, or cerebrospinal fluid at any point during the clinical trial. Circulating anti-rLAS-uPA antibodies were detected in the blood of all dogs by day 14 post-infusion, and these antibodies persisted for the duration of the trial (**Figure 4**).

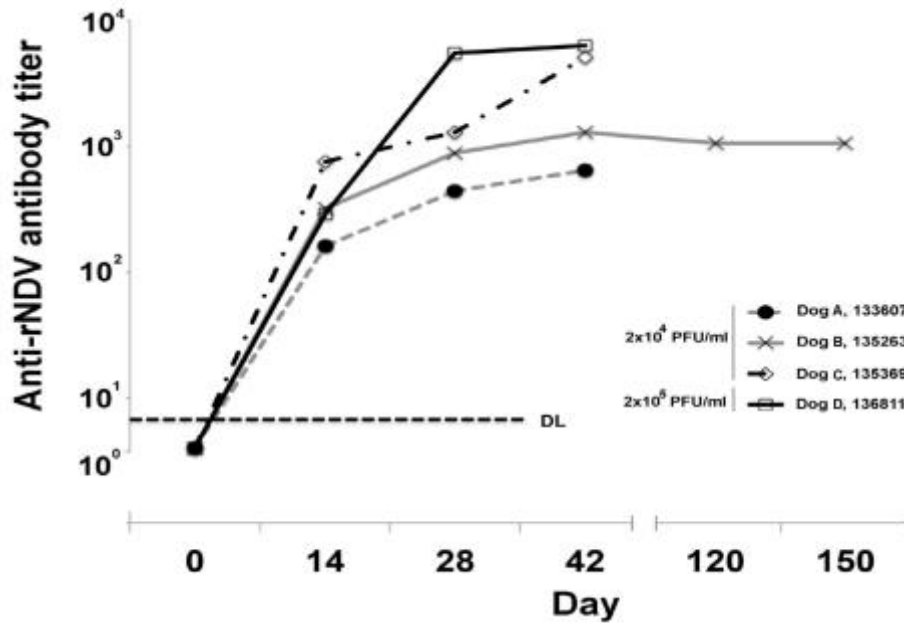


**Figure 4: Anti-rNDV Antibody Responses in Dogs Treated with rLAS-uPA.**

**Key:** DL= detection limit.

Quantification of the cytokines TNF-alpha, IFN-gamma, and TRAIL revealed that in all dogs, serum concentrations of these factors increased significantly and were sustained throughout the duration of the trial compared to baseline ( $P < 0.02$  for all comparisons to baseline; **Figure 5**).

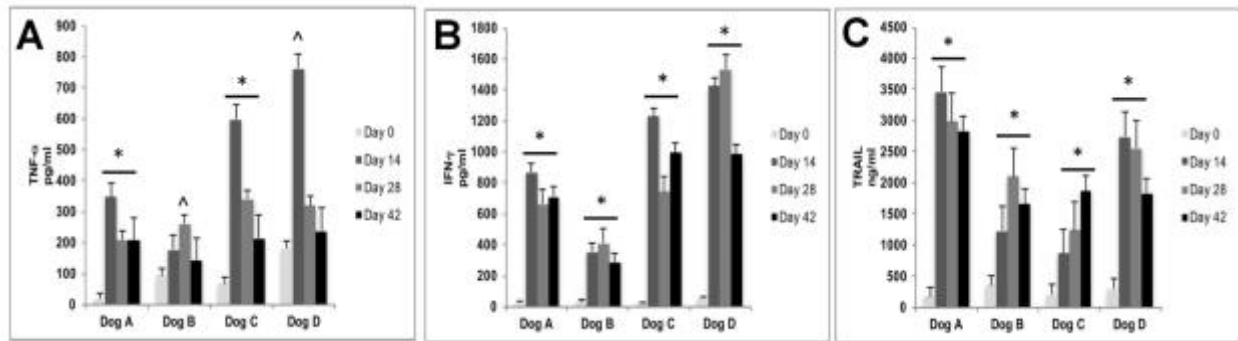


**Figure 5: Serum concentrations of TNF-alpha (A),**

**IFN-gamma (B) and TRAIL (C) in dogs treated with rLAS-uPA.**

**Key:** An asterisk (\*) indicates all post-treatment (Days 14, 28, and 42) concentrations significantly greater than baseline ( $P < 0.02$ ). An up arrow (^) indicates individual time point significantly greater than baseline ( $P < 0.02$ ).

*d. Assessment of Therapeutic Response to rLAS-uPA*

Pre- and post-oncolytic viral treatment MRI of the extra-axial masses were viewed and assessed based upon RAVNO standards.<sup>32</sup> All dog enrolled in the study had a single quantifiable target lesion. A board-certified radiologist, board-certified neurologist, and neurology resident independently analyzed each set of MRI images. No objective evidence of significant changes in overall tumor size were documented from baseline (MRI at enrollment into the clinical trial) to post-treatment MRI acquisition, with all dogs characterized as having stable disease (SD) over the trial period (**Table 7**). Qualitatively, mild changes in the heterogeneity manifesting as cystic regions in the tumors of patient A and patient D were noted by all observers (**Figure 6**).

**Table 7: RAVNO MRI-Based Tumor Response Assessments**

Patient	Pre-treatment 2D Evaluation			Observer Average	Post-treatment 2D Evaluation			Observer Average
	Radiologist	Neurologist	Resident		Radiologist	Neurologist	Resident	
<b>A</b>	43.1 mm	43 mm	43 mm	43 mm	42.7 mm	47 mm	44 mm	44.5 mm
<b>B</b>	14.2 mm	16 mm	13 mm	14.4 mm	17.8 mm	17 mm	14 mm	48.8 mm
<b>C</b>	17.1 mm	19 mm	16 mm	17.3 mm	19 mm 20.9 mm*	21 mm	19 mm 20 mm	19.7 mm
<b>D</b>	25.4 mm	28 mm	24 mm	25.8 mm	25.1 mm	29 mm	26 mm	26.7 mm

**Key:** \*Patient C had 2 post-treatment MRI assessments one at 14 days post-infusion and the other at 119 days post-infusion.

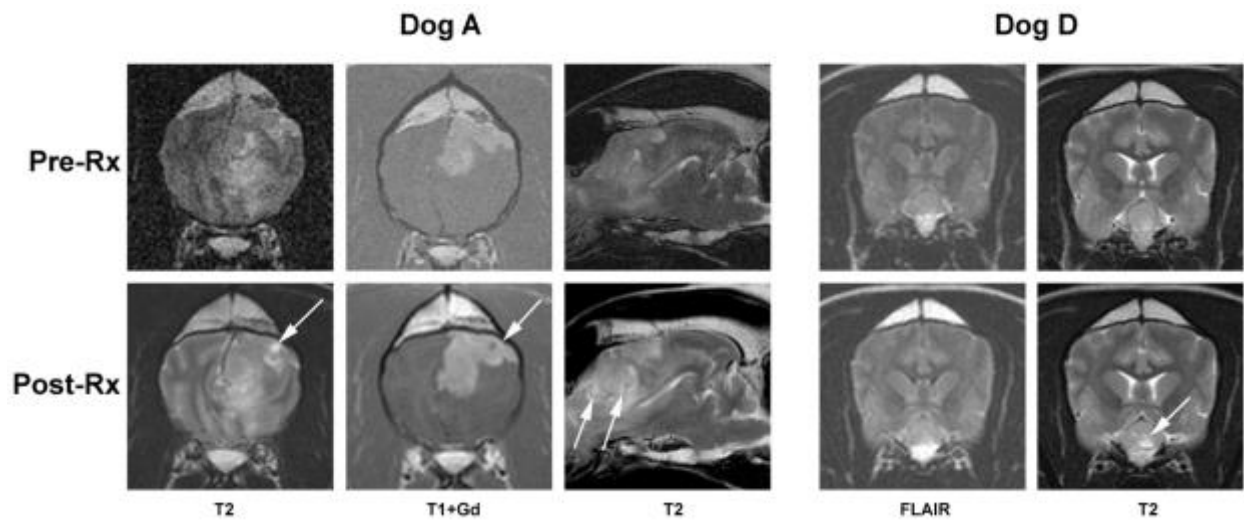


**Figure 6: Comparative pre- and post-treatment MRI images of dogs (patients) A and D demonstrating cystic foci (arrows) in their tumors post-treatment.**

Foci are hyperintense on T2W and FLAIR images and hypointense on T1W post-contrast image (T1+Gd).

The Karnofsky performance scores of all dogs remained static over the course of the trial (Table 7). The progression free survivals and any treatment administered after completing the trial are provided in Table 7. Dogs A and B succumbed of tumor-related complications (structural epilepsy) after completing the trial. At the time of writing, Dogs C and D are still alive.

**Table 8: Clinical Outcomes of Dogs Treated in the Trial**

Patient	Karnofsky Performance Score				Progression Free Survival (Days)	Additional Post-Trial Treatments
	Day 0	Day 14	Day 28	Day 42		
<b>A</b>	75	75	80	N/A <50 at 37 Days	37	Palliation
<b>B</b>	95	95	95	95	242	Palliation
<b>C</b>	95	95	95	95	Alive (>585)	HFIRE Surgical Cytoreduction Fractionated Radiation Therapy
<b>D</b>	90	90	90	90	Alive (>487)	None

Tumor tissue from one dog (patient C) was available for RT-PCR analysis for rLAS-uPA genetic material. rLAS-uPA virus was detected in the surgical resection specimen of the tumor from this case, but not in a blood sample obtained at the time of surgery (**Figure 7**).

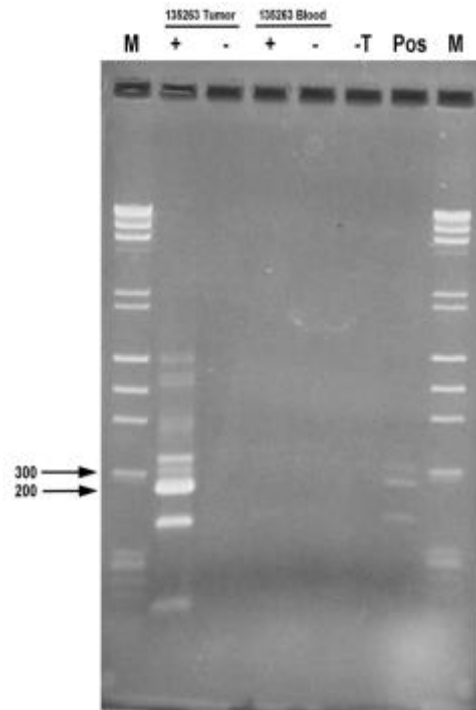


**Figure 7: RT-PCR for rLAS-uPAR NDV in the Tumor and Blood of Patient C.** In the tumor sample, an amplicon of the expected 235 base pair size is observed. Abbreviation Key: M= molecular weight ladder; Pos= positive control; -T = no temperature



## CHAPTER 4: DISCUSSION

The immunohistochemistry data from this study clearly documents that uPAR protein is overexpressed and therefore uPA activity is present in canine meningioma. This provided justification for the development of a recombinant, genetically modified NDV (rLAS-uPA) which could be used as part of a phase I clinical trial to target the urokinase plasminogen activator system directly. This was accomplished by replacing the LaSota fusion (F) protein cleavage site with a uPA cleavage site, so that the F protein would be cleavable exclusively by uPAR.<sup>63</sup> All of the higher-grade tumors (grade II) expressed uPAR protein compared to only the majority (86%) of low-grade (grade I) tumors, which is suggestive of increased activity of the uPA system in more “malignant” tumors. Additionally, the uPAR protein appeared in greater concentration and in more locations throughout the tumor tissue sample in the grade II tumors compared to grade I. These findings correlate positively with previous evaluation that the uPA system plays a supporting role in tumorigenesis and local tissue invasion.

The results of the clinical trial help to bolster the study hypothesis that the intravenous administration of a genetically modified recombinant Newcastle Disease Virus is generally safe and well-tolerated in canines during the immediate peri- and post-infusion time frames. Additional data acquisition is required in order for power-analyses to be relevant and weighted, and it was for this reason that additional data analyses were not performed.

Insufficient data is the main limitation on the interpretation of the results of this clinical trial, as there arose unforeseen complication with the generation of the rLAS-uPA oncolysate mid-way through the trial. Without additional virus, the trial was unable to be completed as designed with a 3+3 dose escalation protocol as previously outlined.

Peri-infusion adverse events were noted in all patients, and were characterized as generalized shivering. The shivering appeared to be self-limiting once the infusion was complete, and may have been attributed to the coolness of the intravenous fluid being administered (thermoregulatory intervention), as well as a possible short-lived, viral related antigen-antibody reaction.<sup>68</sup> Previous NDV trials have documented similar “influenza-like” symptoms in humans infected with an oncolytic strain of the virus, which have been described as fever and malaise.<sup>69</sup>

Seizure activity during the course of the viral infusion trial period was also noted in 3/4 (75%) of patients, which is corroborative of the location of their structural disease. Structural epilepsy is a known disease entity in both canine and human patients and is thought to occur secondary to changes in neuronal membrane excitability and other changes to cerebral metabolism as a result of tumor growth and inflammation. The incidence of epilepsy related to brain tumors in humans is estimated to be 20-40%<sup>70</sup>, this incidence has not been able to be accurately quantified in canine patients. Therefore, the seizure noted in these patients may have been related to their pre-existing disease and related structural epilepsy. However, possible cellular effects of the oncolytic viral infusion cannot be ruled out. These effects can be postulated to include increased local neuroinflammation secondary to apoptosis, and the subsequent development neuronal hypersynchronicity; however, there is a lack of histopathological data to support any lengthy extrapolation.

Post-treatment changes to the inherent tumor Magnetic Resonance Imaging characteristics were noted in 2/4 (50%) dogs (See **Figure 6**, Patient A and Patient D). These changes consisted of small (~1mm diameter) hyperintense foci (on T2W images), and hypointense/heterogeneous foci (On T1W images) as compared to gray matter, within what was observed previously to be a largely homogenous appearing extra-axial mass lesion.

Hyperintensity on T2W imaging is suggestive of fluid (cerebrospinal fluid, edema, tumor infiltration, necrosis, etc.) and is a relatively non-specific finding. Hypointensity on T1W imaging is suggestive of fluid, gas and/or mineralization of the affected structure. However, hyperacute hemorrhage which contains oxyhemoglobin may also appear T1W hypointense, as can vascular structures depending on the rate of blood flow during image acquisition.

Given the appearance of these post-treatment changes it can be hypothesized that tumor necrosis/remodeling secondary to the viral therapy may have been present. Unfortunately, this cannot be confirmed given that no histopathological data is available (patient D still alive). Additionally, assessment of data from human clinical trials using lentogenic Newcastle Disease Virus and other viral oncolysates, has shown that patients develop coagulative necrosis on post-treatment histopathological evaluation.<sup>69</sup>

Humoral immune responses were documented in 4/4 dogs (100%) with evidence of anti-rLAS-uPA antibodies present in circulation by day 14, as well as increased circulation of INF- $\alpha$  and tumor necrosis factor alpha (TNF- $\alpha$ ). Viral recovery was negative in all patients regardless of progression through the trial (receipt of multiple doses of viral oncolysate). Previous studies in both murine<sup>71</sup> and human models<sup>72</sup> have shown that NDV infected macrophages exert a potent tumoricidal effect in vitro by induction of apoptosis in target cells. This apoptotic pathway is mediated primarily by interaction of members of the TNF/TRAIL superfamily. This canine clinical trial is supportive of similar TNF activity, given the increase in circulating TNF alpha and TRAIL noted within circulation of all trial patients.

INF alpha was also noted to be increased in the patient population. This cytokine has been historically shown to be an important host signaling mechanism identifying viral and/or bacterial invasion and aiding in inhibition of disease replication. Elevation in blood INF alpha

levels is supportive of an innate and likely contributive to a humoral immune response (especially given the fact that anti-NDV antibodies were noted in all patients on subsequent sample assessment).

Given the lack of infectious recovery and evidence of circulating antibody response, it is suspected that the immune system of each patient was able to decrease the effectiveness of the viral infusion from at least day 14 onwards. Prior NDV oncolytic trials in humans were able to document viral recovery throughout the treatment trial period.<sup>69</sup> Stronger evidence either in favor of, or against the efficacy of this treatment to reach its intended target tissue across the blood brain barrier is lacking at this time. Only 1/4 dogs (25%) underwent tumor burden assessment (Patient C). Analysis states that the tissue collected was positive for NDV, and therefore is definitive for target tissue penetration; however, additional data is needed in order to better define the true importance of this targeting in vitro.

Given the results of the study, alternative dosing interval and intensity would likely have been of benefit to the investigative process in order to have completely ruled-in or ruled-out this therapy as a potential treatment option for intracranial meningioma in the dog.

## CHAPTER 5: CONCLUSIONS AND FUTURE DIRECTIONS

The results of this abbreviated clinical trial showed that intravenous infusion of rLAS-uPA is well-tolerated in the dog at 20,000 pfu/mL and 200,000 pfu/mL. Completion of the second dosing cohort and initiation of a third dosage escalation would have been helpful in better determining the viral infusate's safety margin in a canine population, as well as have aided in better understanding of treatment efficacy. As at this time we cannot effectively answer the question: Is treatment efficacy dose dependent? Although the author is aware that other factors are also likely involved (such as definitive tumor identification, tumor size, etc.) Administration of an increased viral dosage (greater than 200,000 pfu/mL) would have helped eliminate the question that the dog's host immune response overpowered the effectiveness of the virus to demonstrably induce apoptosis and that the viral dose administered was sub-therapeutic.

Virus was recoverable from single enrollee's tumor tissue sample. Tissue sample collection from each patient in order to look for virus and uPA expression would have been helpful to provide greater weight to the single-sample proof that the virus targets tissue in-vivo as hypothesized.

All canines developed virus neutralizing antibodies by day 14 of treatment trial. Prior viral-therapy studies have shown that tolerization, which is the administration of small amounts of viral antigen into the host's body in order to help "tolerize" that individual's immune system to a specific virus, may help to prevent antibody formation. Tolerization was not utilized in this trial given the preliminary investigation of the rLAS-uPA in canines, but may be helpful for future investigations. Administration of additional virus prior to the 14-day window (for instance

smaller doses of virus administered every 3 days for a total of 200,000 pfu/mL, versus larger doses which may run the risk of developing dose-related toxicity that has not yet been proven, etc.) could potentially also increase the effectiveness of therapy, as the trial showed that there was a lack of significant antibody production in the individual dog's immune systems prior to day 14.

In order to better identify rLAS-uPA as the correct oncolytic viral therapy for use in intracranial meningioma, conformation of tumor type is vital to further investigations and would require pre-treatment biopsy with histopathology which would increase cost of treatment, patient morbidity and also raise questions regarding the ethicality of small biopsy versus surgical resection which is proven treatment option for intracranial meningioma. Overall, the viral therapy shows promise but there remain many unanswered questions and the efficacy of this treatment modality is unproven.

## REFERENCES

1. Veterinary cooperative oncology group (2011). Veterinary cooperative oncology group - common terminology criteria for adverse events (VCOG-CTCAE) following chemotherapy or biological antineoplastic therapy in dogs and cats v1.1. *Veterinary and Comparative Oncology*. doi:10.1111/j.1476-5829.2011.00283.x
2. Ostrom, Q. T., Gittleman, H., et al. (2016). CBTRUS Statistical Report: Primary Brain and Other Central Nervous System Tumors Diagnosed in the United States in 2009–2013. *Neuro Oncol* 18 (suppl\_5): v1-v75. doi: 10.1093/neuonc/nov207
3. Ostrom, Q. T., Gittleman, H., et al. (2015). CBTRUS Statistical Report: Primary Brain and Central Nervous System Tumors Diagnosed in the United States in 2008-2012. *Neuro Oncol*, 17 Suppl 4, iv1-iv62. doi:10.1093/neuonc/nov189
4. Sessums, K., & Mariani, C. (2009). Intracranial meningioma in dogs and cats: a comparative review. *Compend Contin Educ Vet*, 31(7), 330-339.
5. Motta, L., Mandara, M. T., & Skerritt, G. C. (2012). Canine and feline intracranial meningiomas: an updated review. *Vet J*, 192(2), 153-165. doi: 10.1016/j.tvjl.2011.10.008
6. Troxel, M. T., Vite, C. H., et al. (2004). Magnetic resonance imaging features of feline intracranial neoplasia: retrospective analysis of 46 cats. *J Vet Intern Med*, 18(2), 176-189.
7. Bentley, R. T. (2015). Magnetic resonance imaging diagnosis of brain tumors in dogs. *Vet J*, 205(2), 204-216. doi: 10.1016/j.tvjl.2015.01.025
8. Csatory, L. K., Gosztanyi, G., et al. (2004). MTH-68/H oncolytic viral treatment in human high-grade gliomas. *J Neurooncol*, 67(1-2), 83-93.
9. Bondy, M., & Ligon, B. L. (1996). Epidemiology and etiology of intracranial meningiomas: a review. *J Neurooncol*, 29(3), 197-205.
10. Oakley, R., & Patterson, J. (2003). Tumors of the central and peripheral nervous system. In D. Slatter (Ed.), *Textbook of Small Animal Surgery* (pp. 2405-2425). Philadelphia Elsevier Science
11. Criscuolo GR. (1993). The genesis of peritumoral vasogenic brain edema and tumor cysts: a hypothetical role for tumor-derived vascular permeability factor. *The Yale Journal of Biology and Medicine*. 66(4):277-314.
12. Lee, J. H. (2008). *Meningiomas: Diagnosis, treatment, and outcome*. London: Springer.

13. Sturges, B. K., Dickinson, P. J., et al. (2008). Magnetic resonance imaging and histological classification of intracranial meningiomas in 112 dogs. *J Vet Intern Med*, 22(3), 586-595. doi:10.1111/j.1939-1676.2008.00042.x
14. Umansky, F., Shoshan, Y., Rosenthal, G., Fraifeld, S., & Spektor, S. (2008). Radiation-induced meningioma. *Neurosurg Focus*, 24(5), E7. doi:10.3171/FOC/2008/24/5/E7
15. Lusi, E. A., Scheithauer, et al. (2012). Meningiomas in pregnancy: a clinicopathologic study of 17 cases. *Neurosurgery*, 71(5), 951-961. doi:10.1227/NEU.0b013e31826adf65
16. Perry, A., Cai, D. X., et al. (2000). Merlin, DAL-1, and progesterone receptor expression in clinicopathologic subsets of meningioma: a correlative immunohistochemical study of 175 cases. *J Neuropathol Exp Neurol*, 59(10), 872-879.
17. Snyder, J. M., Shofer, F. S., Van Winkle, T. J., & Massicotte, C. (2006). Canine intracranial primary neoplasia: 173 cases (1986-2003). *J Vet Intern Med*, 20(3), 669-675.
18. McEntee, M. C., & Dewey, C. W. (2013). Tumors of the nervous system. In S. J. Withrow, D. M. Vail, & R. L. Page (Eds.), *Withrow and MacEwen's Small Animal Clinical Oncology* (Vol. 5, pp. 583-596). St. Louis: Elsevier Inc.
19. Adamo, P. F., Cantile, C., & Steinberg, H. (2003). Evaluation of progesterone and estrogen receptor expression in 15 meningiomas of dogs and cats. *Am J Vet Res*, 64(10), 1310-1318.
20. Patnaik A, Kay W, Hurvitz A(1986). Intracranial meningiomas: A comparative pathological study of 28 dogs. *Vet Pathol* 369–373
21. Jagannathan, J., Oskouian, R. J., Yeoh, H. K., Saulle, D., & Dumont, A. S. (2008). Molecular biology of unresectable meningiomas: implications for new treatments and review of the literature. *Skull Base*, 18(3), 173-187. doi:10.1055/s-2007-1003925
22. Meuten, D. (Ed.). (2017). *Tumors in domestic animals* (Fifth edition. ed.). Ames, Iowa: John Wiley & Sons.
23. Nakayama H, Okumichi T, Nakashima S. et al. (1997). Papillary adenocarcinoma of the sigmoid colon associated with psammoma bodies and hyaline globules: report of a case. *J. Clin. Oncol.* 27 (3): 193-6. doi:10.1093/jjco/27.3.193
24. Tonn J, Westphal M, Rutka JT. (2009). *Oncology of CNS Tumors*. Springer Verlag. ISBN:364202873X.



25. Wisner, E. R., Dickinson, P. J., & Higgins, R. J. (2011). Magnetic resonance imaging features of canine intracranial neoplasia. *Vet Radiol Ultrasound*, 52(1 Suppl 1), S52-61. doi:10.1111/j.1740-8261.2010.01785.x
26. Rossmeisl, J. H., Kopf, K., & Ruth, J. (2015). Magnetic Resonance Imaging of Meningiomas Associated with Transcalvarial Extension through Osteolytic Skull Defects in a Cat and Two Dogs. *Journal of Veterinary Medicine and Research*, 2(3).
27. Mercier, M., Heller, H. L., Bischoff, M. G., Looper, J., & Bacmeister, C. X. (2007). Imaging diagnosis--hyperostosis associated with meningioma in a dog. *Vet Radiol Ultrasound*, 48(5), 421-423.
28. Axlund TW, McGlasson ML, Smith AN. (2002). Surgery alone or in combination with radiation therapy for treatment of intracranial meningiomas in dogs: 31 cases (1989-2002). *J Am Vet Med Assoc* 221:1597–1600.
29. Greco JJ, Aiken SA, Berg JM, et al. (2006). Evaluation of intracranial meningioma resection with a surgical aspirator in dogs: 17 cases (1996–2004). *J Am Vet Med Assoc*. 229:394–400.
30. Kaley T, Barani I, Chamberlain M, et al. (2014). Historical benchmarks for medical therapy trials in surgery- and radiation-refractory meningioma: a RANO review. *Neuro-Oncology*. 16(6):829-840. doi:10.1093/neuonc/not330.
31. Rossmeisl J. H. (2014). New treatment modalities for brain tumors in dogs and cats. *Vet Clin North Am Small Anim Pract* 44:1013–1038.
32. Klopp, L.S. and Rao, S. (2009). Endoscopic-Assisted Intracranial Tumor Removal in Dogs and Cats: Long-Term Outcome of 39 Cases. *Journal of Veterinary Internal Medicine*, 23: 108–115. doi:10.1111/j.1939-1676.2008.0234.x
33. Ijiri, A., Yoshiki, K., Tsuboi, S., Shimazaki, H., Akiyoshi, H., & Nakade, T. (2014). Surgical resection of twenty-three cases of brain meningioma. *J Vet Med Sci*, 76(3), 331-338
34. Hu, H., Barker, A., Harcourt-Brown, T., & Jeffery, N. (2015). Systematic Review of Brain Tumor Treatment in Dogs. *J Vet Intern Med*, 29(6), 1456-1463. doi:10.1111/jvim.13617
35. Rossmeisl JH, Jones JC, Zimmerman K, Robertson J. (2013). Survival time following hospital discharge in dogs with palliatively treated primary brain tumors. *J Am Vet Med Assoc*, 242(2): 193-198. PMID: 23276095

36. Alexander, D.J. (1991) Newcastle disease and other paramyxo virus infections. In B.W. Calnek, H.J. Barnes, C.W. Beard, W.M. Reid & H.W. Yoder Jr. (Eds.), *Diseases of Poultry* 9th edn (pp. 496–519). London: Wolfe Publishing
37. Al-Garib, S. O.; Gielkens, A.L.J., Gruys, E., & Koch, G. (2003). Review of Newcastle disease virus with particular references to immunity and vaccination. *World Poult. Sci. J.*, 59, 185–200.
38. Kapczynski D. R., Afonso C. L. and Miller P. J. (2013). Immune responses of poultry to Newcastle disease virus. *Dev. Comp. Immunol.* 41:447-453.  
<http://dx.doi.org/10.1016/j.dci.2013.04.012>
39. Bhaiyat, M.I., Ochiai, K., Itakura, C., Islam, M.A. & Kida, H. (1993). Brain lesions in young broiler chickens naturally infected with amesogenic strain of Newcastle disease virus. *Avian Pathology*, 23,693–708.
40. Spindler, K. R., & Hsu, T. H. (2012). Viral disruption of the blood-brain barrier. *Trends Microbiol*, 20(6), 282-290. doi:10.1016/j.tim.2012.03.009
41. Qiu, X., Fu, Q., Meng, C., et al. (2016). Newcastle Disease Virus V Protein Targets Phosphorylated STAT1 to Block IFN-I Signaling. *PLoS One*, 11(2), e0148560.  
doi:10.1371/journal.pone.0148560
42. Ravindra, P. V., Tiwari, A. K., Ratta, B., Chaturvedi, U., Palia, S. K., Subudhi, P. K., . . . Chauhan, R. S. (2008). Induction of apoptosis in Vero cells by Newcastle disease virus requires viral replication, de-novo protein synthesis and caspase activation. *Virus Res*, 133(2), 285-290. doi:10.1016/j.virusres.2008.01.010
43. Elankumaran S, Rockemann D, Samal SK. Newcastle disease virus exerts oncolysis by both intrinsic and extrinsic caspase-dependent pathways of cell death. *J. Virol* 2006; 80:7522–7534.
44. Elankumaran, S., V. Chavan, et al. Type I interferon-sensitive recombinant newcastle disease virus for oncolytic virotherapy. *J Virol* 2010; 84(8): 3835-3844
45. Dock, G. (1904). The influence of complicating diseases upon leukemia. *Am J Med Sci* 127, 563-592.
46. Kelly E., Russell S.J. History of oncolytic viruses: genesis to genetic engineering. *Mol. Ther.* 2007;15:651–659.

47. Lorence, R. M., Roberts, M. S., O'Neil, J. D., Groene, W. S., Miller, J. A., Mueller, S. N., & Bamat, M. K. (2007). Phase 1 clinical experience using intravenous administration of PV701, an oncolytic Newcastle disease virus. *Curr Cancer Drug Targets*, 7(2), 157-167.
48. Walter, R. J., Attar, B. M., Rafiq, A., Tejaswi, S., & Delimata, M. (2012). Newcastle disease virus LaSota strain kills human pancreatic cancer cells in vitro with high selectivity. *JOP*, 13(1), 45-53.
49. Walter, R. J., Attar, B. M., Rafiq, A., Delimata, M., & Tejaswi, S. (2012). Two avirulent, lentogenic strains of Newcastle disease virus are cytotoxic for some human pancreatic tumor lines in vitro. *JOP*. 13(5), 502-513. doi:10.6092/1590-8577/977
50. Toyoda, T., Sakaguchi, T., Hirota, H., Gotoh, B., Kuma, K., Miyata, T., & Nagai, Y. (1989). Newcastle disease virus evolution. II. Lack of gene recombination in generating virulent and avirulent strains. *Virology*. 169(2), 273-282.
51. Krishnamurthy, S., Takimoto, T., Scroggs, R. A., & Portner, A. (2006). Differentially regulated interferon response determines the outcome of Newcastle disease virus infection in normal and tumor cell lines. *J Virol*. 80(11), 5145-5155. doi:10.1128/JVI.02618-05
52. Steiner HH, Bonsanto MM., et al. (2004). Anti-tumor vaccination of patients with glioblastoma multiforme in a case-control study: feasibility, safety and clinical benefit. *J Clin Oncol*. 22: 4272–4281.
53. *Abdullah, J.M., Ideris, A., & Mustafa, Z. (2014). Newcastle Disease Virus Interaction in Targeted Therapy against Proliferation and Invasion Pathways of Glioblastoma Multiforme. BioMed research international.*
54. Biswas M, Johnson JB, Kumar SR, et al. Incorporation of host complement regulatory proteins into Newcastle disease virus enhances complement evasion. *J Virol* 2012; 86(23): 12708-12716
55. Ferguson, M. S., Lemoine, N. R., & Wang, Y. (2012). Systemic delivery of oncolytic viruses: hopes and hurdles. *Adv Virol*, 2012, 805629. doi:10.1155/2012/805629
56. Bai, A., Higham, E., Eisen, H. N., Wittrup, K. D., & Chen, J. (2008). Rapid tolerization of virus-activated tumor-specific CD8+ T cells in prostate tumors of TRAMP mice. *Proc Natl Acad Sci USA*, 105(35), 13003-13008. doi:10.1073/pnas.0805599105

57. Choong PF, Nadesapillai AP (2003) Urokinase plasminogen activator system: a multifunctional role in tumor progression and metastasis. *Clin Orthop Relat Res* (415 Suppl):S46–S58.
58. Blaisi, F., Carmeliet, P. (2002). uPAR: a versatile signalling orchestrator. *Nat. Rev., Mol. Cell Biol.*, 3, 932–943
59. Duffy MJ (2004) The urokinase plasminogen activator system: role in malignancy. *Curr Pharm Des* 10(1):39–49
60. Gouri A., Dekaken A., et al. (2016). Plasminogen activator system and breast cancer: potential role in therapy decision making and precision medicine. *Biomark Insights* 11:105–111
61. Carmeliet, P., Moons, L., et al. (1997). Urokinase-generated plasmin activates matrix metalloproteinase during aneurysm formation. *Nat. Gen.*, 17, 439–444
62. Reith A., Rucklidge G. J., (1992). Invasion of brain tissue by primary glioma: evidence for the involvement of urokinase-type plasminogen activator as an activator of type IV collagenase. *Biochem Biophys Res Commun* 186(1): 348-354
63. Salajegheh, M., Rudnicki, A., & Smith, T. W. (2005). Expression of urokinase-type plasminogen activator receptor (uPAR) in primary central nervous system neoplasms. *Appl Immunohistochem Mol Morphol*, 13(2), 184-189.
64. Rossmeisl, J. H., Robertson, J. L., et al. (2017). Expression and activity of the urokinase plasminogen activator system in canine primary brain tumors. *Oncotargets and Therapy*, 10, 2077-2085
65. Thomson, S. A., Kennerly, E., et al. (2005). Microarray analysis of differentially expressed genes of primary tumors in the canine central nervous system. *Vet Pathol*, 42(5), 550-558. doi:10.1354/vp.42-5-550
66. Rossmeisl JH, Garcia PA, Daniel GB, et al. (2014). Invited review-neuroimaging response assessment criteria for brain tumors in veterinary patients. *Vet Radiol Ultrasound* 55(2),115-132.
67. Di Terlizzi R, Platt S (2006) The function, composition and analysis of cerebrospinal fluid in companion animals: Part I - Function and composition. *Vet J* 172: 422-431. doi:10.1016/j.tvjl.2005.07.021. PubMed: 16154365.

68. Hirayama, F. (2013). Current understanding of allergic transfusion reactions: incidence, pathogenesis, laboratory tests, prevention and treatment. *British Journal of Haematology*, 160(4), 434–444. <http://doi.org/10.1111/bjh.12150>
69. Freeman, Arnold I., Zichria Zakay-Rones, John M. Gomori, Eduard Linetsky, Linda Rasooly, Evgeniya Greenbaum, Shira Rozenman-Yair, Amos Panet, Eugene Libson, Charles S. Irving, Eithan Galun, Tali Siegal, Phase I/II Trial of Intravenous NDV-HUJ Oncolytic Virus in Recurrent Glioblastoma Multiforme, *Molecular Therapy*, Volume 13, Issue 1, January 2006, Pages 221-228, ISSN 1525-0016, <https://doi.org/10.1016/j.ymthe.2005.08.016>
70. Maschio, M. (2012). Brain Tumor-Related Epilepsy. *Current Neuropharmacology*, 10(2), 124–133. <http://doi.org/10.2174/157015912800604470>
71. Umansky, V., V. A. Shatrov, V. Lehmann, V. Schirmacher. 1996. Induction of NO synthesis in macrophages by Newcastle disease virus is associated with activation of nuclear factor- $\kappa$ B. *Int. Immunol.* 8: 491
72. Washburn, B., M. A. Weigand, A. Grosse-Wilde, M. Janke, H. Stahl, E. Rieser, M. R. Sprick, V. Schirmacher, and H. Walczak. 2003. TNF-related apoptosis-inducing ligand mediates tumoricidal activity of human monocytes stimulated by Newcastle disease virus. *J. Immunol.* 170:1814-1821